Published in "Bulletin de la Société Géologique de France
179(3): 297-314, 2008" which should be cited to refer to this work.

Surface processes versus kinematics of thrust belts: impact on rates of erosion, sedimentation, and exhumation – Insights from analogue models

CÉCILE BONNET[1], JACQUES MALAVIEILLE[2] and JON MOSAR[1]

Key-words. – Analogue modelling, Alpine orogenic wedge, Surface processes, Material trajectories, Uplift/Exhumation.

Abstract. – The mechanical equilibrium of an orogenic wedge is maintained thanks to interactions between tectonic processes and surface processes. To better constrain the influence of erosion and sedimentation on the evolution of orogens, we performed a series of analogue models based on the tapered wedge principle, varying the amounts of erosion and sedimentation. The models develop by frontal accretion in the foreland basin and by simple underthrusting and subsequent underplating in the hinterland. The variations in rates of erosion and sedimentation strongly modify the extent, the morphology, the structures, the timing of development and the material paths in the different models. Under certain conditions, entire structural units can be formed and subsequently eroded out of the geological record, leading to important underestimations when restoring sections. Particles located in the converging lower-plate or in the upper-plate show complex uplift paths related to tectonic stages. The correlation between models and three Alpine tectonic cross-sections emphasizes the role of erosion and sedimentation on the dynamics and development of the orogen and adjacent Molasse basin. Along strike changes in the present structure of the orogen could be explained in part by differences in surface processes.

Interactions tectonique-érosion-sédimentation dans un avant-pays de chaîne. Modèles analogiques et comparaison aux Alpes

Mots-clés. – Modélisation analogique, Prisme orogénique alpin, Processus de surface, Trajectoires de matière, Soulèvement/Exhumation.

Résumé. – L'équilibre mécanique d'un prisme orogénique dépend des interactions entre les processus tectoniques et les processus de surface. Afin de mieux contraindre l'influence de l'érosion et de la sédimentation sur l'évolution d'un orogène, nous avons réalisé une série de modèles analogiques de prismes d'accrétion, au cours desquels les taux d'érosion et de sédimentation varient. Les conditions initiales géométriques et cinématiques de la modélisation tiennent compte de l'hétérogénéité rhéologique liée à l'héritage structural, sédimentologique ou mécanique et rencontrée dans la plupart des avants-pays de chaînes. Deux mécanismes tectoniques principaux agissent dans le prisme, l'accrétion frontale et le sous-placage. L'érosion et la sédimentation conditionnent en interaction les transferts de matière. Le développement de chevauchements en séquence au front implique également les dépôts syntectoniques du bassin d'avant-pays. Simultanément, l'accrétion par sous-placage se manifeste essentiellement par des mouvements verticaux et la formation de duplex accommodant le raccourcissement dans les domaines plus internes du prisme. Les variations du ratio érosion/sédimentation influent fortement sur la structure tectonique des modèles, la cinématique, les transferts de matière et l'exhumation au sein du prisme. Les implications structurales sont nombreuses. Par exemple, au cours de l'évolution d'une chaîne, des unités structurales entières sont érodées et peuvent disparaître hors de l'enregistrement sédimentaire, conduisant à d'importantes sous-estimations des taux de raccourcissement lors de la restauration de coupes tectoniques. Des particules situées dans des unités tectoniques différentes suivent des trajectoires d'enfouissement et d'exhumation complexes, directement contrôlées par ces interactions tectonique – processus de surface. La comparaison entre les modèles et trois coupes tectoniques dans l'avant-pays Alpin met en valeur le rôle de l'érosion et de la sédimentation sur la dynamique du front de l'orogène et le développement du bassin molassique. Une partie des changements structuraux observés le long de l'axe de la chaîne, pourrait correspondre à une réponse tectonique différente liée aux variations dans les processus de surface.

INTRODUCTION

Based on theoretical models, it has been shown that orogens commonly adopt a distinct geometry with a low-tapered pro-wedge facing the subducting plate, and a high-tapered retro-wedge on the internal side [Beaumont *et al.*, 1992; Willett *et al.*, 1993; Pfiffner *et al.*, 2000; Naylor *et al.*, 2005]. The tapered wedge geometry is established because

1. Department of Geosciences – Earth Sciences, University of Fribourg, Chemin du Musée 6, 1700 Fribourg, Switzerland. cecile.bonnet@unifr.ch ; jon.mosar@unifr.ch
2. Geosciences Montpellier, Université Montpellier II, Place Eugène Bataillon, 34095 Montpellier cedex 5, France. jacques.malavieille@gm.univ-montp2.fr

orogens tend to be on the verge of internal failure along potential slip planes [Davis *et al.*, 1983]. According to these models, the velocity field of the crust and, hence, the exhumation paths of rock particles, depends on erosion at the surface [e.g., Horton, 1999; Persson and Sokoutis, 2002]. Consequently, any changes in erosion rates potentially result in a modification of the strain pattern [Schlunegger and Hinderer, 2001] and thus the internal evolution of the wedge. Based on these ideas, we performed a series of analogue experiments including erosion and sedimentation to investigate the foreland/hinterland evolution of a mountain wedge. Using a simple set-up we investigate the influence of erosion and sedimentation on the internal structure of the wedge while maintaining a constant taper angle. The models are designed to allow a direct comparison to the setting and tectonic evolution of the western Alps. They can explain the first order tectonic structures present in convergent orogenic settings, taking into account the structural and stratigraphic heritage present in subducting continental margin lower-plates in order to simulate realistic conditions of a deforming plate margin edge such as the Alpine Helvetic domain. Our aim is threefold:

– to better understand the impact of erosion/sedimentation changes on the tectonic structure and the evolution of an orogenic wedge such as the Alps,

– to analyse the role played by former structural heritage in the tectonic evolution, and

– to determine the relative influence of these parameters on the main tectonic events recorded in the foreland during the evolution of the orogenic belt.

The results of our modelling allow us to draw conclusions on the kinematic evolution of the Alpine foreland (structural development, basin evolution, exhumation, etc) and to suggest a link between the along strike changes in the geometry of the orogen and variations in the intensity of surface processes.

ANALOGUE MODELLING

A series of seventeen experiments was performed during the study. The basic geometric setup simulates a section of a growing orogen in a convergent system, when the orogenic lid upper-plate begins to override the subducting lower-plate formed by pre-structured basement and cover units (fig. 1). This pre-structured setup is justified since we want to investigate the inversion of a former passive margin setting and marginal basin realm such as formed by the Ultrahelvetic and the Helvetic domains. During the orogenic evolution of the Alps the inversion of the Ultrahelvetic tilted block margin leads to the formation of the Flysch basin, whereas the inversion of the platform-type marginal basin of the Helvetic leads to the formation of the Molasse basin [Stampfli and Marthaler, 1990]. Such domains are typically composed by half-graben like basins controlled by the tilted blocks of the margin [Trümpy, 1980; Wildi *et al.*, 1989; Funk and Loup, 1992]. It is important to consider these existing geometries and mechanical weaknesses, even in a simplified way, to allow meaningful comparisons between modelling results and the Alpine orogeny. The location of the main features (faults and basins) is based on various reconstructions, but mainly on work by Burkhard and Sommaruga [1998], Stampfli *et al.* [1998] and Stampfli *et al.* [2002]. Eleven preliminary experiments have led to settle all the details of both the basic model and the experimental procedure, as presented in the following. The first order geometry and mechanical behaviour of the different tectonic units and depositional realms have been constrained by successive improvements to achieve a model that can serve as a good analogue of the European Alpine margin and the Alps. Then to better understand the impact of surface processes on thrust wedge growth, six experiments (numbered 42 to 47) were performed with variable rates of sedimentation and erosion.

Experimental set up, basic model and experimental procedure

The initial geometry and rheologic structure of the basic model (fig. 2) has been designed using data from a restored section across the western Alps proposed by Burkhard and Sommaruga [1998]. The lengths of units, angles, rheologies and location of décollement levels in the experiments are directly constrained by their results. The classical sandbox device (fig. 2) we used is close to the set up of Malavieille [1984] and Konstantinovskaia and Malavieille [2005]. It is made by a flat basal plate bound by two lateral glass walls.

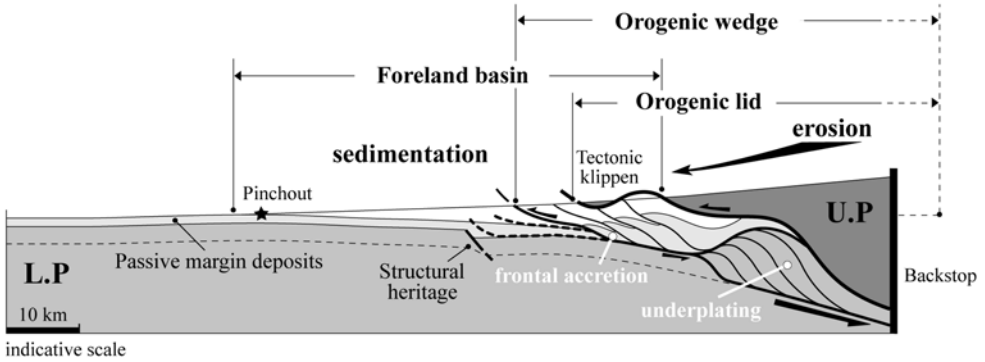

FIG. 1. – Interactions between surface processes (erosion/sedimentation) and tectonics in a foreland system. The orogenic lid is dark grey, the foreland basin white and the converging lower-plate (basement + cover) is light grey. U.P = upper-plate and L.P = lower-plate. Frontal accretion and underplating control the orogenic growth.

FIG. 1. – *Système d'avant-pays illustrant les interactions entre les processus de surface (érosion/sédimentation) et la tectonique. Le « traîneau écraseur » orogénique apparaît en gris foncé, le bassin d'avant-pays en blanc et la plaque inférieure convergente (socle + couverture) en gris clair.* U.P = *plaque supérieure et* L.P = *plaque inférieure. L'accrétion frontale et le sous-placage contrôlent la croissance de l'orogène.*

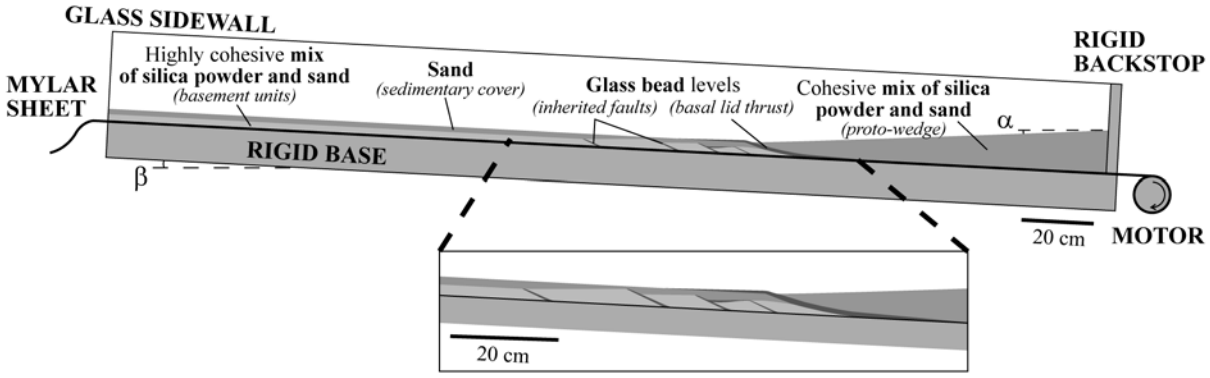

FIG. 2. – Experimental sandbox device and basic model of a growing orogen and its foreland basin, based on a model Coulomb wedge (on the scheme, surface α dips 2° to the left and base β 3° to the right). Pre-structured analogue materials are pulled on a Mylar sheet against a rigid backstop, leading to the development of a thrust wedge. On the right side, the upper-plate consists in a homogeneous solid lid (blue) that will override on a basal thrust (red) the lower-plate constituted by a succession of solid basement units (pink) and their more "deformable" cover (green), both pre-structured by inherited faults (red). (Electronic version appears in colour)

FIG. 2. – *Appareillage de modélisation et modèle de base d'un orogène en croissance et de son bassin d'avant-pays, (sur le schéma, la surface α plonge de 2° vers la gauche et la base β de 3° vers la droite). Les matériaux analogues convergent vers une butée rigide, créant un prisme chevauchant. Sur la partie droite, un matériau granulaire homogène (bleu) constitue la plaque supérieure qui va chevaucher (rouge) la plaque inférieure constituée par une succession d'unités cohésives (socle rose) et de leur couverture plus « déformable » (vert), les deux étant pré-structurés (structures héritées en rouge). (Version électronique en couleur)*

A motor pulls a 10 cm wide Mylar sheet with a rough (high basal) friction surface.

Analogue materials deposited on the Mylar sheet are accreted against the rigid backstop during convergence developing a thrust wedge. The backstop simulates the undeformed part of the upper-plate lithosphere (no tectonic output is allowed during the experiment). Cohesion and size are scaled (scaling, with a factor of 10^5, and characterization of model materials are discussed in Gutscher *et al.* [1998], Gutscher *et al.* [1996], Kukowski *et al.* [2002], Lallemand *et al.* [1994] and Lohrmann *et al.* [2003]). The basal plate length is 280 cm. It offers a maximum convergence of 160 cm (equivalent to about 400 km at the scale of a natural orogenic wedge). One camera records all stages of the experiment allowing to do structural interpretations and semi-quantitative analyses.

The "critical wedge" theory [Davis *et al.*, 1983; Dahlen, 1984; Dahlen *et al.*, 1984] predicts that the geometry of a growing wedge (defined by its surface slope α and its basal slope β) is a function of the material strength and the basal friction. The surface of the model Coulomb wedge (α) used in the experiments (fig. 2) dips 2º to one side and its base (β) dips 3º into the opposite direction (angle of subduction). In models, these angles have been chosen based on Alpine sections discussed in Mosar [1999] and Lacombe and Mouthereau [2002]. Two natural boundary conditions have been simplified in the models: the lithospheric flexure is not considered (the flat basal plate was simply tilted to reach the mean basal slope angle) and, assuming the possibility of thrusts to develop at a mid-crustal detachment level [Burkhard and Sommaruga, 1998], only the part of the model equivalent to the upper-part of the crust can be involved in the deformation. Thus, in our setting, part of the model lower-plate is forced to detach along the Mylar sheet during shortening. Despite small variations in length and thickness of some given layers, the six experiments described here are built with the same initial configuration. Two main units compose the models: on the right side (fig. 2), the homogeneous orogenic lid represents the upper-plate that overrides, on the left side, a succession of pre-cut basement units and their cover that form the subducting plate. The analogue granular materials have frictional properties satisfying the Coulomb theory [Davis *et al.*, 1983; Dahlen, 1984; Dahlen *et al.*, 1984] and they mimic a non-linear deformation behaviour of crustal rocks in the brittle field [Lohrmann *et al.*, 2003]. The orogenic lid is made of a cohesive mix of silica powder and sand. The aeolian sand used in this study is rounded with a grain size of 200 to 315 μm and a density of 1700 kg/m^3. The internal coefficient of friction is 0.57 and the cohesion Co = 20 Pa. The pure dry silica powder has a significantly higher cohesion (150 Pa) than sprinkled sand (20 Pa), allowing the simulation of stronger (more resistant) material. The lid is separated from the subducting plate by a glass bead layer (thickness < 8 mm) that simulates a former basal thrust. Glass beads have a grain size between 50 and 105 μm and are a Coulomb material of density similar to that of dry sand but, due to their close to perfect roundness, their coefficient of internal friction is about 23% smaller (0.44), with almost zero cohesion. The basement units of the lower-plate are also composed of sand and silica powder, but with a higher proportion of the latter to model stronger lithologies encountered in a crystalline basement. They are pre-cut by thin layers of glass beads simulating inherited normal faults with shallow to intermediate dip. These weak zones bordering old basins can be reactivated as reverse faults during the compression. Finally, a layer of sprinkled sand represents the sedimentary cover of the subducting plate. The novelty of our approach is consequently that the analogue model takes into account both the tectonic and stratigraphic inheritance of the subducting margin.

Except for experiment 42, in all other experiments we performed both erosion and sedimentation. Even when varying the rates of the surface processes, the experimental procedure was based on the assumption that the tectonic development of the model governs the rates and locations of erosion and sedimentation. In each experiment (except 42), erosion and sedimentation rates were imposed to maintain the initially chosen mechanical equilibrium of the wedge

($\alpha+\beta = 5^o$ as discussed prior). Erosion is performed by hand with a thin metal plate (the sand being removed using a vacuum cleaner) both on the lid and on the recently deposited materials to maintain the slope of the wedge at a constant angle (on average we attempted to maintain slopes of 2-4°). Sedimentation is performed by sprinkling sand. Simultaneously in the foreland, the successive layers of basin fill are added to reach the chosen equilibrium profile. Erosion of the units was applied in a constant manner, independently of their lithological nature, as a function only of topography. Thus higher topographies and topographic anomalies were eroded leading to erosion that is distributed and linearly dependant on elevation. Generally this means that erosion is increasing towards higher topographies. This is supported by other analogue models [Hoth *et al.*, 2004; Konstantinovskaia and Malavieille, 2005], and also by observations from natural situations where erosion can be positively correlated with elevation [Summerfield, 1994; Hooke, 2003]. The varying qualitative rates of imposed erosion and sedimentation are indicated for the six described experiments (fig. 7). Overall the erosion/sedimentation budget is not balanced in the sense that much more material is removed out of the system than is deposited (output > input). This is equivalent to the natural situation in the Alpine foreland basin, where more than half of the sediments have been carried out of the system by large rivers into the neighbouring sinks that are the Black sea, North sea and Mediterranean sea [Kuhlemann, 2000; Kuhlemann *et al.*, 2001; Kuhlemann *et al.*, 2002]. The erosion/sedimentation budgets in the experiments follow those estimated from the Alps.

Several experiments present minor differences with the initial set up (fig. 3) of the basic model adopted. In experiment 42, basement units and cover form two flat, parallel

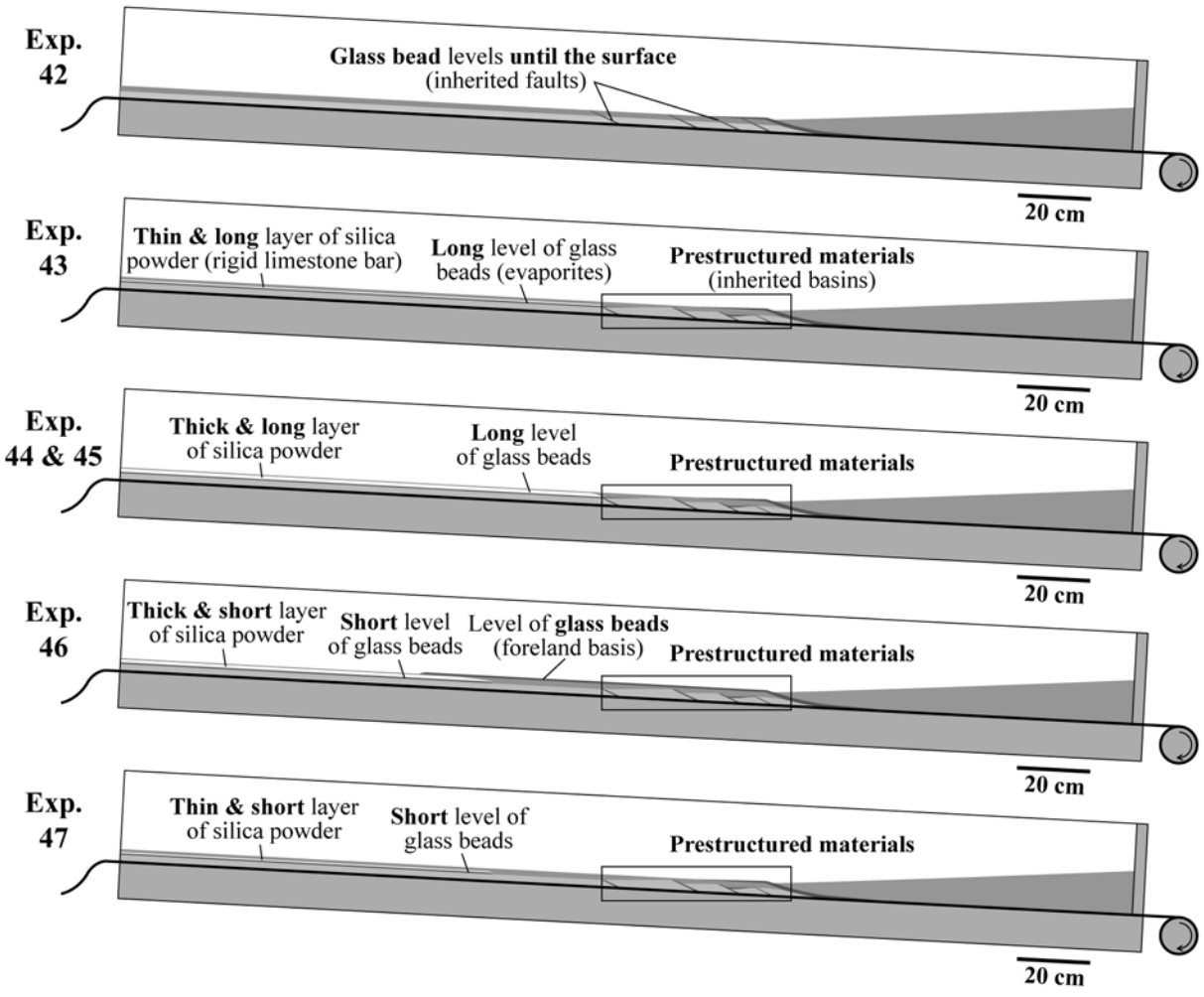

FIG. 3. – Initial set up of the six presented experiments. The internal part of the converging lower-plate is either pre-structured by inherited basins cutting only the basement or by inherited faults reaching the surface (red levels). With the exception of experiment 42, a cohesive layer (white) simulating a rigid lithology is placed in the core of the cover, underlined by a weak level (red) of same length simulating evaporites at the base of the cover. The thickness and length of this cohesive layer vary depending on the experiment. In the experiment 46, a glass bead level is added on the right half of the cover's length to simulate a major weakness at the base of the future foreland basin. (Electronic version appears in colour)

FIG. 3. – *Structure initiale des six expériences présentées. La partie interne de la plaque inférieure convergente est soit pré-structurée par des bassins hérités affectant uniquement le socle, soit par des failles héritées atteignant la surface (niveaux rouges). À l'exception de l'expérience 42, une couche cohésive (blanc), simulant une lithologie rigide, est placée au cœur de la couverture et est soulignée par un niveau de faiblesse (rouge) de même longueur, simulant des évaporites à la base de la couverture. L'épaisseur et la longueur de cette couche cohésive varient selon l'expérience. Dans l'expérience 46, un niveau de microbilles est ajouté sur la moitié droite de la couverture afin de simuler une zone majeure de faiblesse à la base du futur bassin d'avant-pays. (Version électronique en couleur)*

layers. The thin levels of glass beads located in the lower-plate cut the basement units, but also the sedimentary cover to finally reach the surface. In contrast, in all the other experiments, the basement top is not flat, and basement units are offset along normal faults forming the inherited basins filled with the sedimentary cover. Except in experiment 42, we introduced in the sedimentary cover of the lower-plate a flat layer of pure silica powder to simulate a high strength lithologic layer that mimics the thick and massive limestone series marking the late Jurassic sediments of the Alpine foreland. A thin level of glass beads (thickness < 2 mm) with the same length than the layer of silica powder is also placed between the basement and the cover of the subducting plate. It mimics a weak layer of evaporites acting as a décollement level. The length of both the silica powder and the glass bead levels varies following the experiments as well as the thickness of silica powder (see dimensions fig. 3). In experiment 46, we added a level of glass beads (thickness < 2 mm) on the right half of the cover's length to simulate a major unconformity at the base of the future foreland basin. This level favours the overriding of the lid on the lower-plate. The final stages of this experiment (46) present an orogenic wedge geometry which is in good agreement with the structure of the present day section across the western Alps [Burkhard and Sommaruga, 1998] at the origin of our basic model. In addition, in the experiment 46 we performed more detailed analyses (sediment budget, evolution in length of the basin, exhumation paths of analogue materials, etc). The evolution of this reference experiment is described below in more details.

Main stages of the reference experiment

To simplify the description of the experiments, we chose to characterize the displacement of the subducting plate in terms of time increments. For instance, the reference experiment (46) is run between the time increments t_0 and t_{38}, for a total shortening of 152 cm (corresponding to 380 km at the natural scale). The key stages of the tectonic evolution are shown in figure 4 with the structural interpretation draped on the pictures.

Shortening in the model induces overriding of the lid onto the top of the basement ramp. The geometrical response is a continuous and marked internal deformation of the lid mainly accommodated by diffuse backthrusting (t_{10} fig. 4). As the orogen starts developing some relief (t_6) and until the end of the experiment, we remove analogue materials in excess (erosion) and deposit sand to maintain a constant wedge slope. The displacement of the orogenic front is first accommodated by several small thrust slices in the foreland sediments, very close to the lid front (t_{10}). The deformation then propagates to the foreland (t_{13}) through the glass bead level located at the base of the sedimentary deposits that is activated as a décollement. The displacement of the orogenic front is accommodated by backthrusting (t_{16}). From the stage t_{16}, the structural heritage controls the deformation of the subducting lower-plate. The inherited weaknesses (normal faults) of the basement are activated as reverse faults. Faulting propagates across the basal décollement level and cuts the surface forming a succession of foreland sediment slices. Then the basement imbricates over-thrust one another due to underplating (t_{23}) [e.g. Platt, 1986]. At t_{29}, the homogeneous part of basement lower-plate (without structural heritage) is spontaneously underplated. The resulting thrust affects the sedimentary cover and the overlying foreland sediments initiating the development of a new foreland fold-and-thrust belt far from the former front. The combined effect of tectonics and erosion leads to a localising of the exhumation on basement units. Then, subsequent uplift isolates the front of the lid forming now a synformal klippen nappe constituted by former imbricated thrust units (t_{29}). The final evolution is marked by the development of the fold-and-thrust belt in the foreland (t_{38}), that allows widening of the orogenic wedge. At this stage, the different units have been largely eroded and more particularly the foreland basin and the orogenic lid including its frontal klippe. The underplating of the basement units has led to the formation of an antiformal nappe stack.

RESULTS OF MODEL ANALYSIS AND TECTONIC IMPLICATIONS

When erosion and sedimentation operate in the experiments (as described previously), the resulting wedge presents a classical geometry of mountain belt with a basement nappe stack in the internal zones and a foreland domain characterized by imbricate thrusting. The two types of tectonic mechanisms involved (frontal accretion and underplating) will be described based on the reference experiment. Then, all the experiments performed with surface processes will be compared to the one without to investigate the influence of erosion and sedimentation on orogenic wedge evolution. Independent variations in rates of erosion and sedimentation strongly modify the structural development of the wedge. To highlight the diversity of geometries obtained, three structural profiles across the western to the central Alpine arc will be compared to model sections. To characterize burial and exhumation of tectonic units during the development of the thrust wedge, we will describe the complex two-dimensional trajectories of particles located in the different tectono-sedimentary units of the model. Finally, material paths obtained from experiments performed with and without surface processes will be compared.

Frontal accretion vs. underplating

Two main types of tectonic mechanisms act simultaneously in the experiments run with surface processes (experiments 43 to 47). In the external parts, frontal accretion leads to the development of a foreland thrust belt, while underplating in the internal zones results in the formation of an antiformal nappe stack (figs 1 and 5).

Frontal accretion affects the recently deposited foreland sediments and starts very early in the experiments (see stage t_{10} in experiment 46, fig. 4). This mechanism is expressed by the successive activation of frontal thrust slices in the foreland basin and favours the growth of the wedge perpendicularly to the orogenic axis. When the sediments thrust by frontal accretion exceed the initial surface slope ($\alpha = 2^o$) of the wedge, they are eroded. Frontal accretion therefore leads to a cyclic syndeformational removal of an important volume of foreland sediments. For instance, in experiment 46 (fig. 6), the slice of foreland sediments trapped between thrusts 1 and 2, activated respectively at t_{13} and t_{15}, has almost vanished at t_{23}, when a third thrust appears in front. Both in the models and in nature, at an advanced stage of

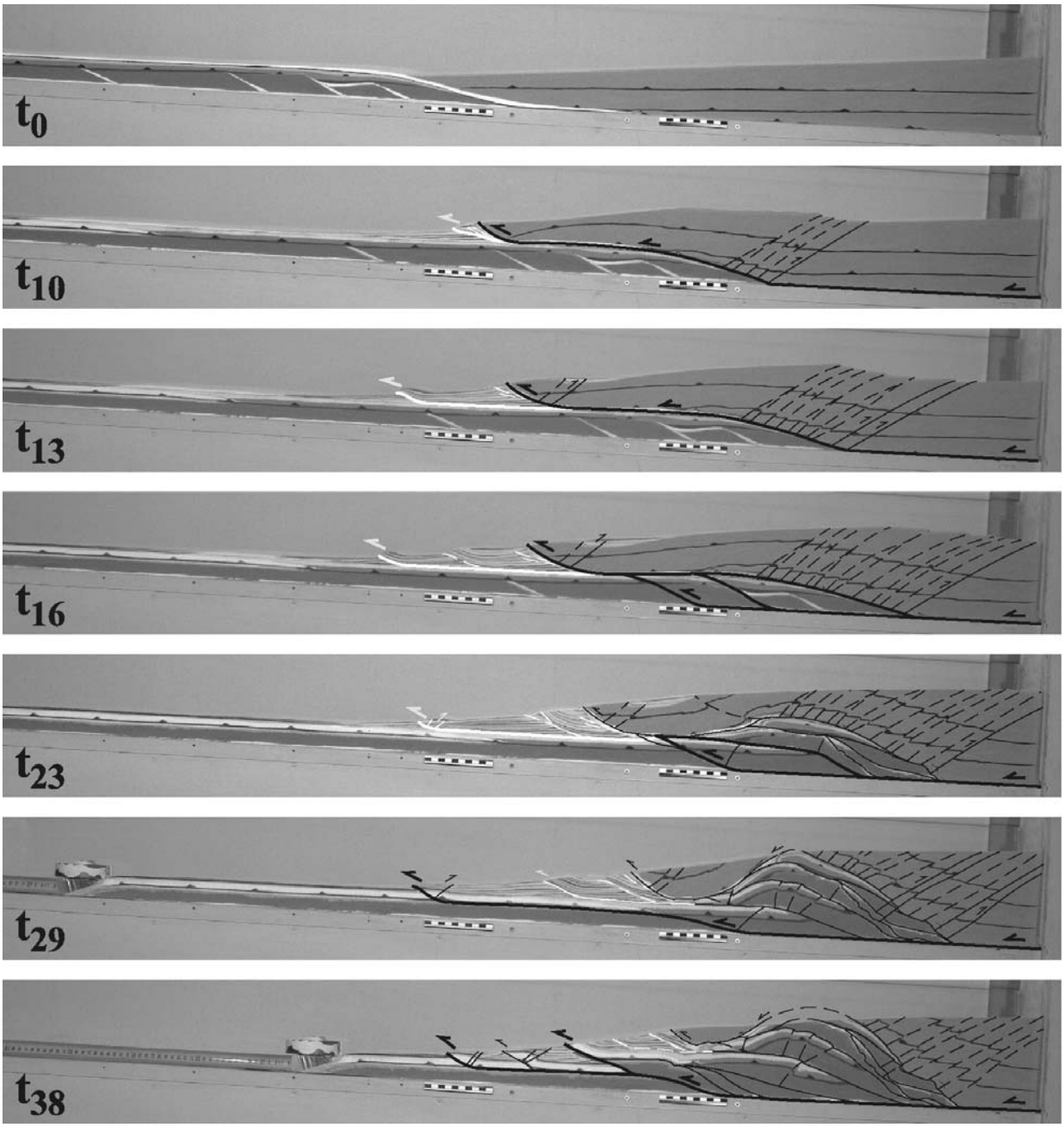

FIG. 4. – Key stages of the reference model evolution from time increment t_0 to t_{38}. Structural interpretation is draped on the pictures: thrusts affecting only the foreland sediments (white), other faults (black), faults accommodating major displacements (thick), minor displacement (thin) and inactive faults (dashed lines). t_0 = initial stage; t_{10} = climb of the lid onto the top of the basement ramp; t_{13} = first slice of foreland sediments; t_{16} = inversion of the inherited basement normal faults and second foreland sediment slice; t_{23} = underplating of the basement imbricates and third slice; t_{29} = spontaneous underplating of the homogeneous part of the basement, initiation of a fold-and-thrust development in the foreland and detachment of a nappe from the lid due to the uplift of basement units; t_{38} = final stage showing the developed foreland fold-and-thrust belt, the remains of the detached nappe and the antiformal basement nappe stack.

FIG. 4. – *Étapes clés de l'évolution du modèle de référence entre les incréments de temps t_0 et t_{38}. L'interprétation structurale est drapée sur les photographies : chevauchements affectant uniquement les sédiments d'avant-pays (blanc), autres failles (noir), failles accommodant des déplacements majeurs (traits épais), des déplacements mineurs (traits fins) et failles inactives (lignes pointillées).* t_0 = *stade initial;* t_{10} = *montée de la plaque supérieure sur la rampe de socle;* t_{13} = *première écaille de sédiments d'avant-pays;* t_{16} = *inversion dans le socle des failles normales héritées et deuxième écaille de sédiments d'avant-pays;* t_{23} = *sous-placage des imbrications de socle et troisième écaille;* t_{29} = *sous-placage spontané de la partie homogène du socle, initiation d'une chaîne plissée et chevauchante dans l'avant-pays et formation d'une nappe du fait du détachement du front de la plaque supérieure suite au soulèvement des unité de socle;* t_{38} = *stade final montrant le développement de la chaîne plissée et chevauchante d'avant-pays, les vestiges de la nappe détachée et l'empilement antiforme de nappes de socle.*

evolution, a number of structures accommodating some displacement are totally eroded. This is the case for thrusts 1 and 2, whose small remnants observable at stage t_{23} (fig. 6) do not provide any indication on the original shape and length of the vanished units. Such a gap in the geologic record created by permanent erosion of tectonic structures

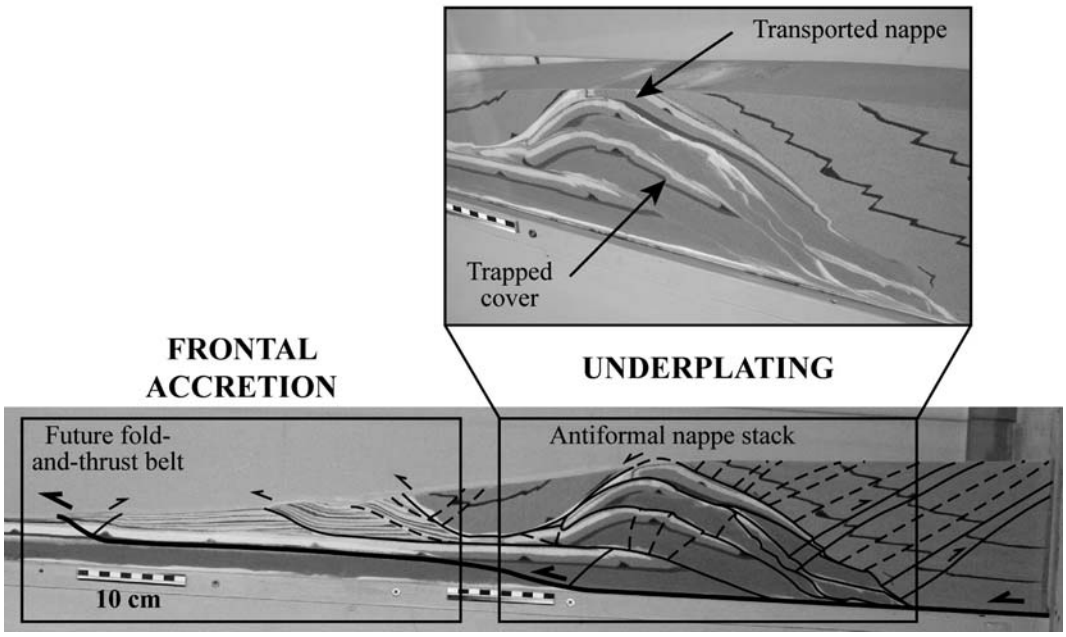

FIG. 5. – Tectonic mechanisms involved in the development of an orogenic wedge: frontal accretion of foreland sediments in the external parts and underplating of basement imbricates in the internal zones. Frontal accretion is initiated early in the experiment (t_{10}) allowing significant erosion of the recently deposited sediments. Underplating starts later (t_{16}) inducing growth of an antiformal nappe stack.

FIG. 5. – *Mécanismes responsables de la croissance du prisme orogénique: accrétion d'unités tectoniques au front du prisme et sous-placage d'imbrications de socle dans les zones internes. L'accrétion frontale s'initie tôt dans l'expérience* (t_{10}) *permettant une importante érosion des sédiments récemment déposés. Le sous-placage débute plus tard* (t_{16}) *et conduit au développement d'un empilement antiforme de nappes de socle.*

may cause major error in the construction of balanced cross-sections, and resulting in large underestimates of the total shortening in mountain belts.

When convergence can no longer be mechanically accommodated by subduction of lower-plate basement units at depth, shortening is taken up by underplating. This mechanism allows material of the subducting lower-plate to be accreted to the upper-plate, contributing to wedge growth. In the experiments, the structural heritage of the lower-plate (weak levels of glass beads in the basement) defines the size of basal duplexes and favours the initiation of underplating, but the process then continues spontaneously in the homogeneous part of the basement due to burial and increasing stress at depth (t_{29} fig. 4). Underplated duplexes lead to the formation of an antiformal nappe stack (fig. 5) where the displacement is accommodated along thrust ramps, favouring localized rapid syn-convergence exhumation. In experiment 46, the geometry of the nappe stack is very close to the one proposed by Burkhard and Sommaruga [1998] for the Alpine crystalline massifs (fig. 10). In their profile, cover units are trapped between the basement imbricates and, similar to the Helvetic nappes, the cover of the two most internal basement units undergoes strong deformation and large tectonic transport.

Variations of erosion and sedimentation rates

A comparison of the experiment without erosion/sedimentation with experiments involving variable rates of erosion/sedimentation, confirms that surface processes play a major role during the evolution of a mountain belt. Models that include erosion/sedimentation and changes in rates of surface processes lead to major structural differences in the orogenic development. Thus, we suggest that the diversity of structural styles and morphologies encountered along the Alpine arc (illustrated by the three cross-sections of figure 10) may be in part a consequence of such regional variations in the intensity of surface processes. The differences in overall amounts of erosion/sedimentation are expressed qualitatively (fig. 7), and are reflected by a wide taper-shaped foreland basin when sedimentation is very high and a narrow one when sedimentation is low. Little erosion (mainly in the hinterland) maintains the orogenic lid and prevents the basement nappes from developing important structural, and subsequently topographic, relief. Significant erosion favours the "rise" of the basement nappe stack, thus enhancing exhumation.

Insights from different experiments

A comparison of six experiments that underwent the same amount of shortening (around 300 km at the natural scale) but variable amounts of sedimentation and erosion (fig. 7) shows a wide range of structures (experiment 42 vs. experiments 43 to 47). Without surface processes (experiment 42), we obtain a classical high friction wedge, i.e. fairly widely spaced frontal imbricate thrusts, with a rather steep frontal slope, and significant shearing occuring along a mid-level detachment, allowing underthrusting of the older imbricate units as observed in similar experiments [Gutscher *et al.*, 1998]. In response to shortening, basement imbricates are first thrust over one another along inherited weaknesses. Then, the unstructured part of the basement spontaneously underthrusts. High erosion (experiment 43) appears to favour the development of steeper basement imbricates in the antiformal stack. In contrast, a very high sedimentation rate (experiment 44, movie 1) strongly inhibits the development

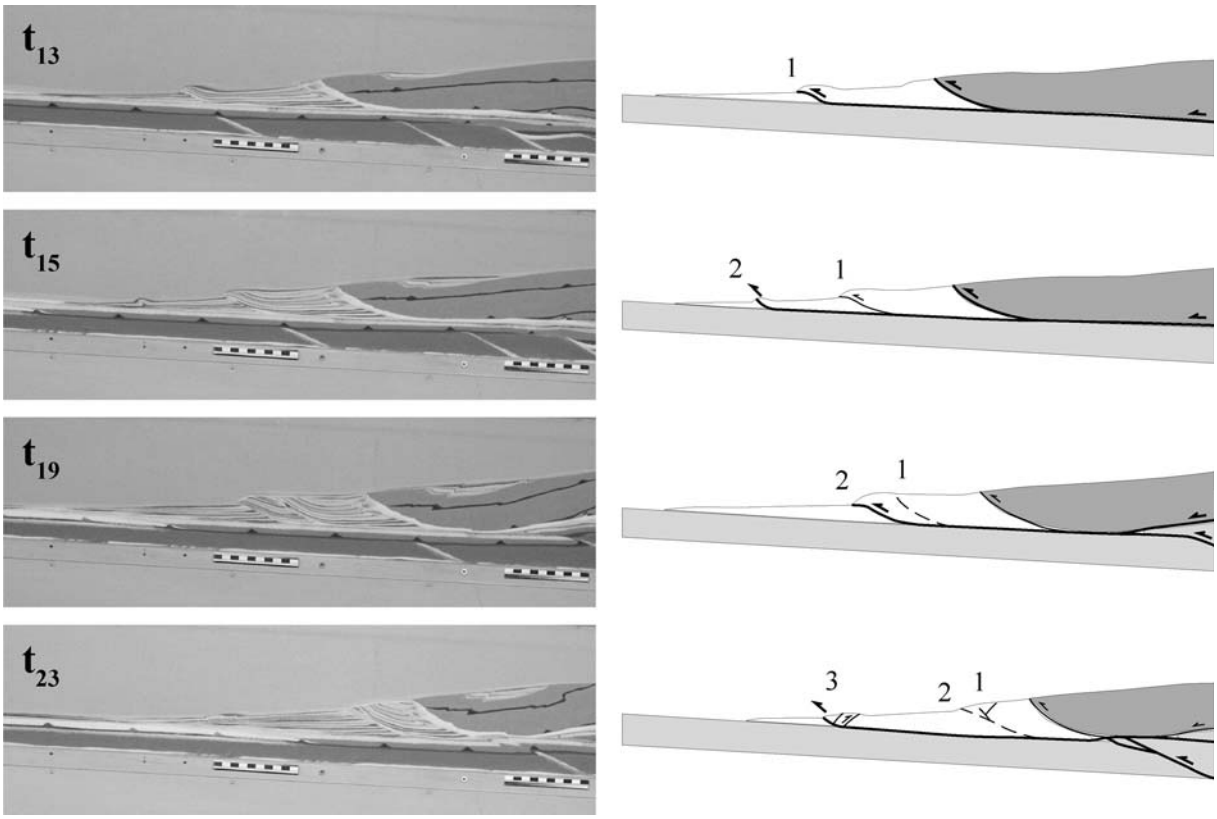

FIG. 6. – Cyclic syndeformational removal of accreted sediments due to constant erosion. Main units and faults are drawn: the lid (dark grey), the basement and cover are grouped (light grey), the foreland sediments (white), the faults accommodating major displacements (thick lines), minor displacement (thin) and the inactive faults (dashed lines). From t_{15}, the foreland sediment slice delimited by thrusts 1 (t_{13}) and 2 (t_{15}) is gradually eroded and when thrust 3 propagates (t_{23}), this tectonic unit has almost disappeared.

FIG. 6. – *L'érosion entraîne l'élimination cyclique et syn-déformationnelle d'une partie des sédiments accrétés dans l'avant-pays. Les unités et failles principales sont dessinées : plaque supérieure (gris foncé), socle et couverture groupés (gris clair), sédiments syntectoniques (blanc), failles accommodant des déplacements majeurs (traits épais), des déplacements mineurs (traits fins) et failles inactives (lignes pointillées). À partir de* t_{15}*, l'écaille de sédiments d'avant-pays délimitée par les chevauchements 1* (t_{13}) *et 2* (t_{15}) *est érodée peu à peu et lorsque le chevauchement 3 se propage* (t_{23})*, cette unité tectonique a pratiquement disparu.*

of such an antiformal stack. In this case, the still horizontal imbricates are underplated on two levels, forming a flat nappe stack. Erosion increases the underplating and focuses the uplift of basement units that constitute a nappe stack. It also favours an important displacement of the cover of the two most internal basement units, overriding the antiformal nappe stack (experiments 43 to 47). This transport (stage A fig. 8) is possibly due to the presence of a décollement level at the base of the cover, similar to the Triassic evaporite level in the Alpine setting.

Very low sedimentation (experiment 43) favours the creation of a number of small thrust slices briefly active in the domain of frontal accretion (fig. 9). High sedimentation results in the development of few long lived thrusts (fig. 9) in the foreland basin sediments (experiments 44, 45 and 47).

Intermediate conditions of sedimentation and erosion (experiment 46) allow exhumation of the basement units and induce the development of both a sedimentary basin and (at an advanced stage of evolution) a new fold-and-thrust belt in the foreland. The focused uplift of the basement nappe stack isolates a klippe from the lid. Low erosion preserves a maximal extent of the lid and consequently favours the preservation of synformal klippen (only experiments 45 and 46). In experiment 46 the nappe overthrusts both the foreland sediments and the antiformal stack. As the sedimentation rate is higher in experiment 45 (movie 2), the klippe lies entirely on foreland basin sediments (stage B fig. 8).

A detailed evolution and quantitative interpretation of the sedimentation/erosion processes and their comparison with the Alpine situation and especially the Alpine foreland basin [Sinclair, 1997; Sissingh, 1997] and its erosional budget [Kuhlemann, 2000] are beyond the scope of this paper and are presented elsewhere [Bonnet, 2007].

Comparison with Alpine cross-sections

Natural orogen-foreland basin systems are not homogeneous along strike due to structural and mechanical heterogeneities, but also due to external parameters such as surface processes. For instance, the width and depth of the north Alpine foreland basin (NAFB) strongly increases along its axis, from SW to NE [Homewood, 1986; Sissingh, 2006a, 2006b], most likely linked to the varying volumes of sedimentary deposits. To better constrain the influence of erosion and sedimentation on the development of the Alps and adjacent northern foreland basin, we compared models with variable rates of surface processes to three Alpine tectonic cross-sections (fig. 10).

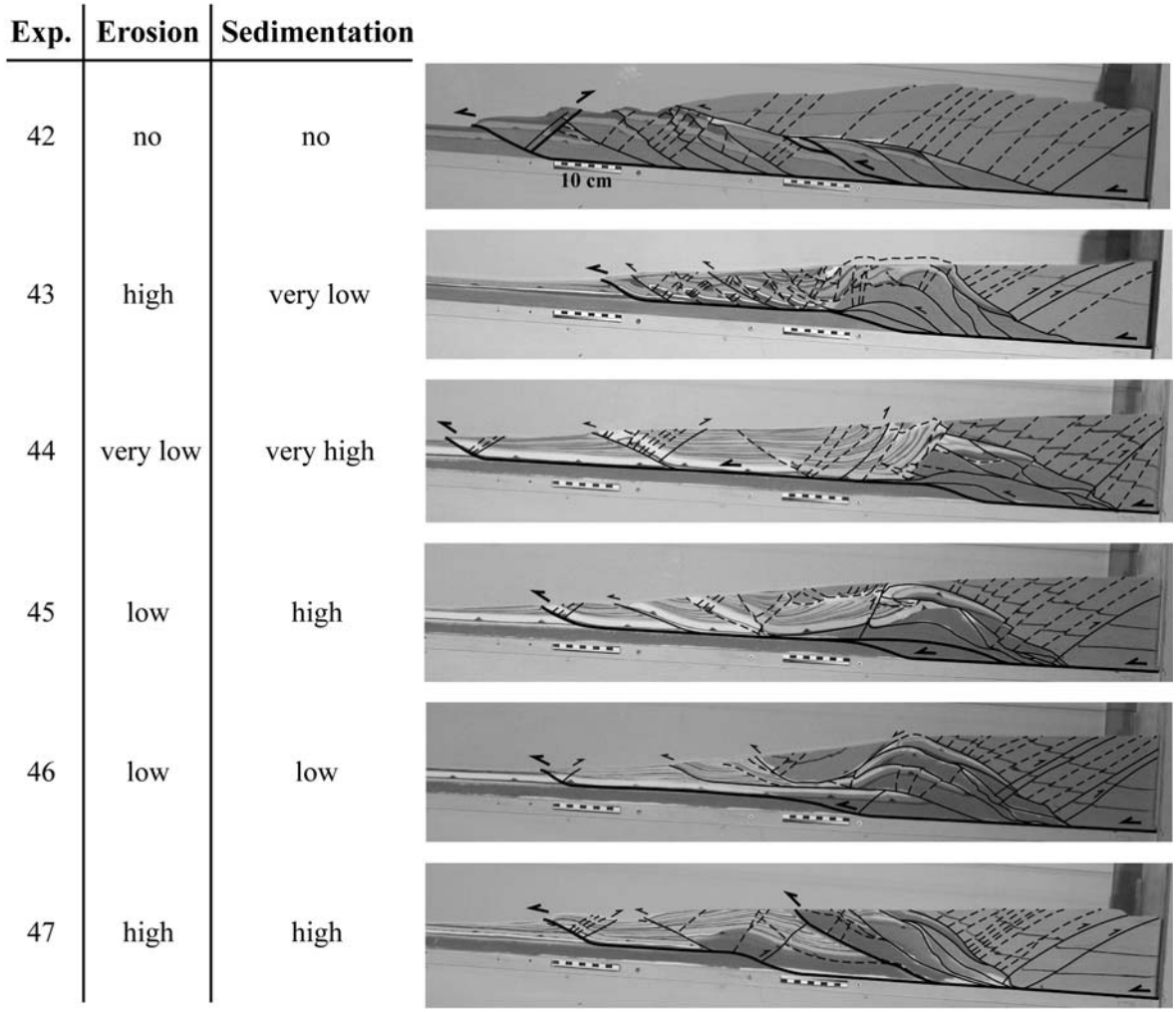

FIG. 7. – Six experiments performed with variable amounts of erosion and sedimentation are compared (for an equal amount of shortening). See legend of figure 6 for fault symbol description. Experiment 42 is a high friction wedge obtained without erosion. Erosion (Exp. 43 to 47) favours underplating and focuses the uplift of basement imbricates. A very low sedimentation (Exp. 43) favours the creation of a number of small thrust slices briefly active in the foreland basin. In contrast, high sedimentation (Exp. 44, 45 and 47) is expressed by few thrusts active for a long time and intense backthrusting. Intermediate conditions of sedimentation and erosion (Exp. 46) lead to a realistic exhumation of the basement units and to the development of both a sedimentary foreland basin and a new, external zone of frontal accretion. Refer to the text for a full description. The additional movies of Exp 43 (movie 1) and Exp 45 (movie 2) illustrate two contrasted conditions of erosion and sedimentation. http://www.sgfr.org/publier/editions/BSGF/Resumes-2008/Res08B3-5.php
Movie 1. – Evolution of a model wedge under high erosion an very low sedimentation (experiment 43).
Movie 2. – Evolution of a model wedge under low erosion an high sedimentation (experiment 45).

FIG. 7. – *Comparatif de six expériences réalisées avec des taux variables d'érosion et de sédimentation (chaque coupe présente le même raccourcissement). Voir la figure 6 pour la description des figurés de failles. Le prisme de l'expérience 42 est obtenu sans érosion. L'érosion (Exp. 43 à 47) accroît le sous-placage et localise le soulèvement des imbrications de socle. Une très faible sédimentation (Exp. 43) favorise la création de nombreuses petites écailles chevauchantes brièvement actives dans le bassin d'avant-pays. Au contraire, une forte sédimentation (Exp. 44, 45 et 47) s'exprime par peu de chevauchements longtemps actifs et affectés par de nombreux rétrochevauchements. Des conditions intermédiaires de sédimentation et d'érosion (Exp. 46) conduisent à une exhumation réaliste des unités de socle et au développement à la fois d'un bassin sédimentaire d'avant-pays et d'une nouvelle zone d'accrétion frontale plus externe. Se référer au texte pour une description complète. Les films additionnels des expériences 43 (animation 1) et 45 (animation 2) illustrent deux conditions d'érosion et sédimentation contrastées.* http://www.sgfr.org/publier/editions/BSGF/Resumes-2008/Res08B3-5.php
Animation 1. – *Évolution d'un modèle soumis à une forte érosion et une très faible sédimentation (expérience 43).*
Animation 2. – *Évolution d'un modèle soumis à une faible érosion et une forte sédimentation (expérience 45).*

In the first model with very low sedimentation and high erosion (experiment 43), the foreland basin is subdivided by thrust-related anticlines into smaller sub-basins. In the western Alps, along a profile from the Jura to the Belledone massif (profile XX' fig. 10), these structures correlate well with anticlines such as the Salève and Ratz. Separated by these narrow sub-basins, the southern border of the folded Jura is located very close to the Alpine front. In the internal part of the foreland, portions of the Molasse basin are overthrust by autochthonous Mesozoic cover such as the Bornes-Aravis massifs. The most external analogue basement imbricates show a rather shallow dip towards the foreland, similar to the northern imbricates of the Belledone massif [Lacombe and Mouthereau, 2002]. Finally, only very small remnants of the Penninic klippen remain both in the model and in the western Alps cross-section (Sulens-Annes klippen).

In the second model with low erosion and sedimentation (experiment 46), the internal part of the foreland basin is disturbed by a succession of small thrusts, comparable to those developed along a more central Alpine profile (profile YY' fig. 10), where the NAFB is an apparently unique basin deep of 3-4 km. Without pre-existing weaknesses, new basement imbricates develop in the frontal part of the analogue wedge, corresponding to a forward evolutionary stage

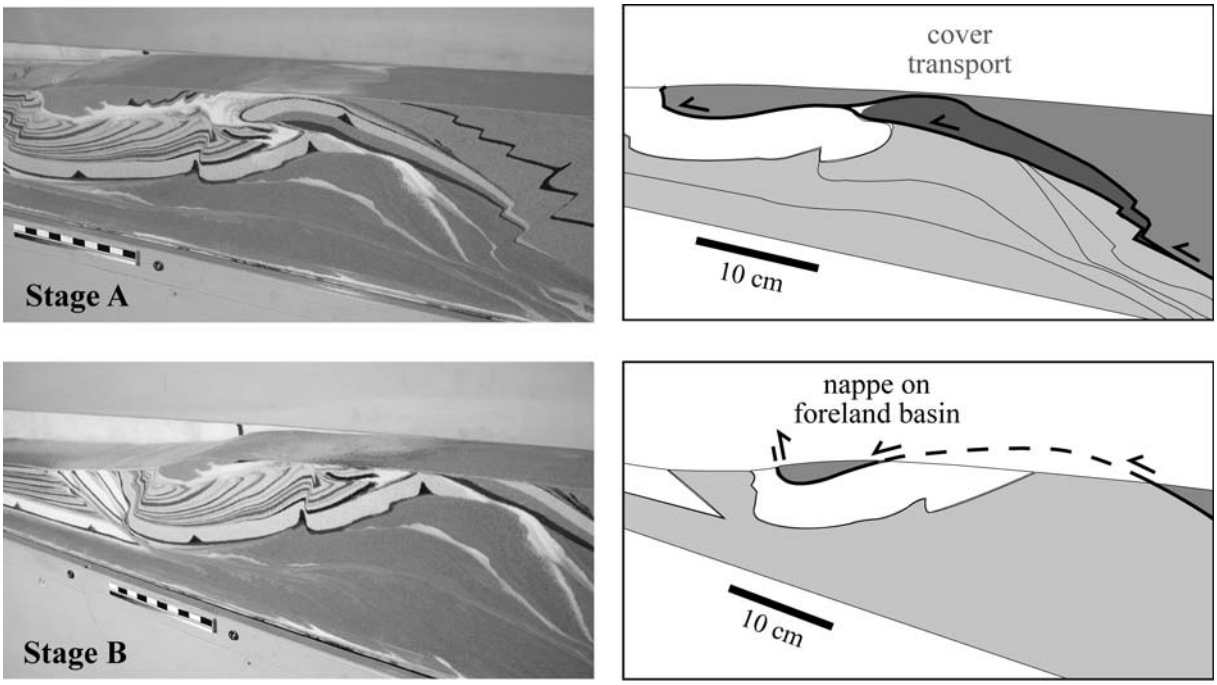

FIG. 8. – At stage A (Exp. 45), the cover (red on the scheme) of the two most internal basement units is transported on top of the antiformal nappe stack. This displacement is possible due to the effect of erosion combined with the presence of a décollement level at the base of the sedimentary cover (Exp. 43 to 47). At stage B, due to the combined effects of low erosion and high sedimentation, the nappe detached of the lid lies only on foreland basin sediments (Exp. 45).

FIG. 8. – *Au stade A (Exp. 45), la couverture (rouge sur le schéma) des deux unités les plus internes de socle est transportée sur le sommet de l'empilement antiforme de nappes. Ce déplacement est possible grâce à l'effet de l'érosion combiné à la présence d'un niveau de décollement à la base de la couverture sédimentaire (Exp. 43 et 47). Au stade B, du fait de l'effet conjugué d'une faible érosion et d'une forte sédimentation, la klippe isolée de la plaque supérieure repose uniquement sur les sédiments du bassin d'avant-pays (Exp. 45).*

of the presumed current Alpine underplating. Autochthonous sedimentary series and foreland basin-sediments (equivalent of the North Helvetic Flysch) are involved in the large basement thrusts bringing basement units (equivalent of the Helvetics external basement) on top of sedimentary cover. Due to the uplift of the antiformal basement nappe stack, the lid cover is separated in two pieces leaving an important allochthonous Penninic klippen equivalent of the Prealpes klippen belt.

In the third model, a broader and thicker foreland basin develops because of high sedimentation associated with high erosion (experiment 47). Similar to the central Alps (profile ZZ' fig. 10), the NAFB reaches its maximum width (more or less 100 km) and thickness (5-6 km). The successive layers of foreland sediment deposits are little deformed, and the layers of molasse remain subhorizontal in the central and northern parts of the basin, and are only affected by steep normal faults. The basement imbrication style is quite different, because the steep imbricates are only slightly underthrust, stay next to one another, and do not constitute an antiformal stack. A frontal basement imbricate develops similarly to model 2 and builds on a triangle structure, as in the central Alps cross-section. Small remnants of the Penninic klippen remain both in the model and in the cross-section, as in model 1.

Results from modelled orogen-foreland basin systems provide insights into the dynamics and development of the Molasse basin and its orogenic hinterland in relation to surface processes. The analogue models suggest that variations along strike of the Alpine structural development depend in part on the different local rates of erosion and sedimentation.

Material transfer

The study of material paths (trajectories) in mountain belts may provide useful insights on their kinematic evolution. Surface processes strongly influence the timing, location and amplitude of rock displacements in the varying members of an orogenic wedge. After a brief outline on exhumation and uplift of rocks, we will study the two-dimensional trajectories of points located in the converging lower-plate and then the differing paths of points located in the upper-plate. The comparison of their trajectories in experiments performed with and without erosion/sedimentation will underscore the influence of surface processes on material transfer in the model wedge.

One way to investigate orogen dynamics is to look at the ages recorded by different thermochronometers across it [Kühni and Pfiffner, 2001; Willett and Brandon, 2002]. To avoid confusion, the terminology used for material displacement during mountain building, follows that of England and Molnar [1990]. Exhumation of rocks means the approaching of a rock particle to the Earth's surface, which is, e.g. recorded by cooling rates calculated from thermochronologic data [e.g., Foster and John, 1999], whereas uplift of rocks means the displacement of rocks with respect to the geoid, or less accurately with respect to the mean sea level.

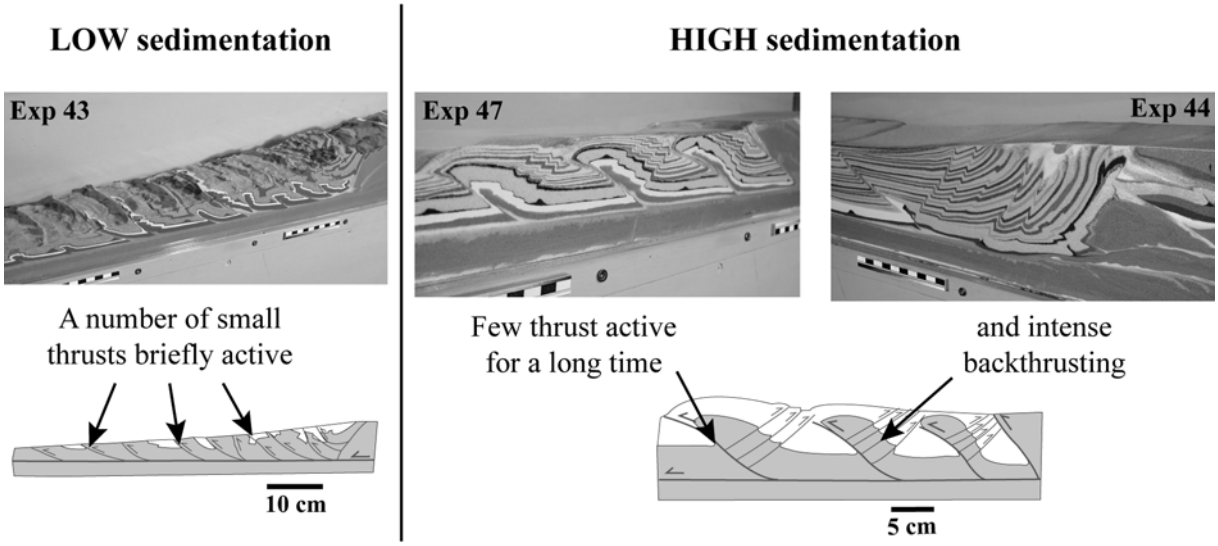

FIG. 9. – Contrasted structures in the foreland due to low or high sedimentation rates.
FIG. 9. – *Structures contrastées dans l'avant-pays dues à des taux faible ou élevé de sédimentation.*

In our study, we have compared the two-dimensional trajectories of five points located in the different members of the model, evolving with or without erosion/sedimentation. In the following, we will first study the trajectories of three points located in the subducting lower-plate and then the paths of two points in the lid. The experimental data are directly scaled to nature in the various graphs to favour a direct comparison with the evolution of a mountain belt. These data may include small errors related to different sources, such as the experimental procedure, the mechanical properties of the used materials and the transition between the device and the graphical representation. However, since these errors are small relative to the size of the studied processes, they can be neglected.

Major experimental tectonic stages through the trajectories of points located in the subducted plate

To describe and investigate the mechanism of underplating leading to the uplift of basement units, the displacement of three points located in the subducting plate is analysed. Two points are chosen at the top of the basement units and a third one inside the cover (fig. 11). The horizontal transport of the points is expressed in terms of incremental displacement relative to a pin, located in the undeformed part of the converging cover (X-axis). The motion of this mobile pin (represented by a white star on the final stage picture) shows the incremental convergence of the lower-plate. The vertical component of displacement (Y-axis) is represented by the depth or elevation of the points to the reference altitude of the pin (dashes on the final stage picture), at the end of the experiment (fig. 11). The location of the studied points has been accurately drawn on pictures of the successive stages of shortening and the displacement in both directions has been systematically measured. Each curve representing the displacement of the described points must be read from right to left, following the orogenic evolution. It appears that the process may be well described in three stages (see pictures fig. 11), each one governed by a major tectonic mechanism. During the phase t_0 to t_{15}, the points are driven to depth quickly due to the subduction of the lower-plate. During the phase t_{16} to t_{28}, the green (C) and the red (B) points undergo a rapid uplift. The blue dot (A) is initially still involved in the subduction, before being uplifted too. The major mechanism responsible for this rapid uplift is the underplating of the basement units, called "Crystalline massifs" in reference to the reference Alpine cross-section. During the t_{29} to t_{38} phase, the uplift of the points slows down. The green (C) and the red (B) dots are completely eroded at the end of the experiment. The major mechanism involved is still the underplating but it now affects the homogeneous and most external part of the basement, called "Autochthonous European foreland basement". The mechanics of the wedge is then modified because deformation propagates toward the foreland. Detailed inspection of the curves shows that the path of two close points (the green (C) and the red (B) ones for instance) does not present exactly the same pattern. While the two points are quickly uplifted between t_{16} and t_{28}, this uplift is not regular (fig. 11). The varying slope of the trajectories indicates the differences in uplift rates of points that may end up very close in a final stage. The secondary variations are linked to the local structural and lithological weaknesses, leading to a different tectonic response.

A different way of investigating transfer of material in mountain belts is the analysis of P,T,t paths. In this case, it is not the displacement of a rock with respect to a fixed reference (corresponding to the uplift) that is measured, but the displacement with respect to the surface (i.e. the exhumation, fig. 12). We decided to express the distance between a rock and the topographic surface in terms of thickness of rocks (including sediments and basement). The distance between a study point and the surface vertically corresponds to the sedimentary thickness (Y-axis fig. 12) measured at each increment of displacement, relative to the pin located in the converging plate (X-axis). For the three points in the subducting lower-plate, the curves representing their two-dimensional displacement measured to a reference altitude (uplift, fig. 11) or to the topographic surface (exhumation, fig. 12) seem to be very similar. The curves

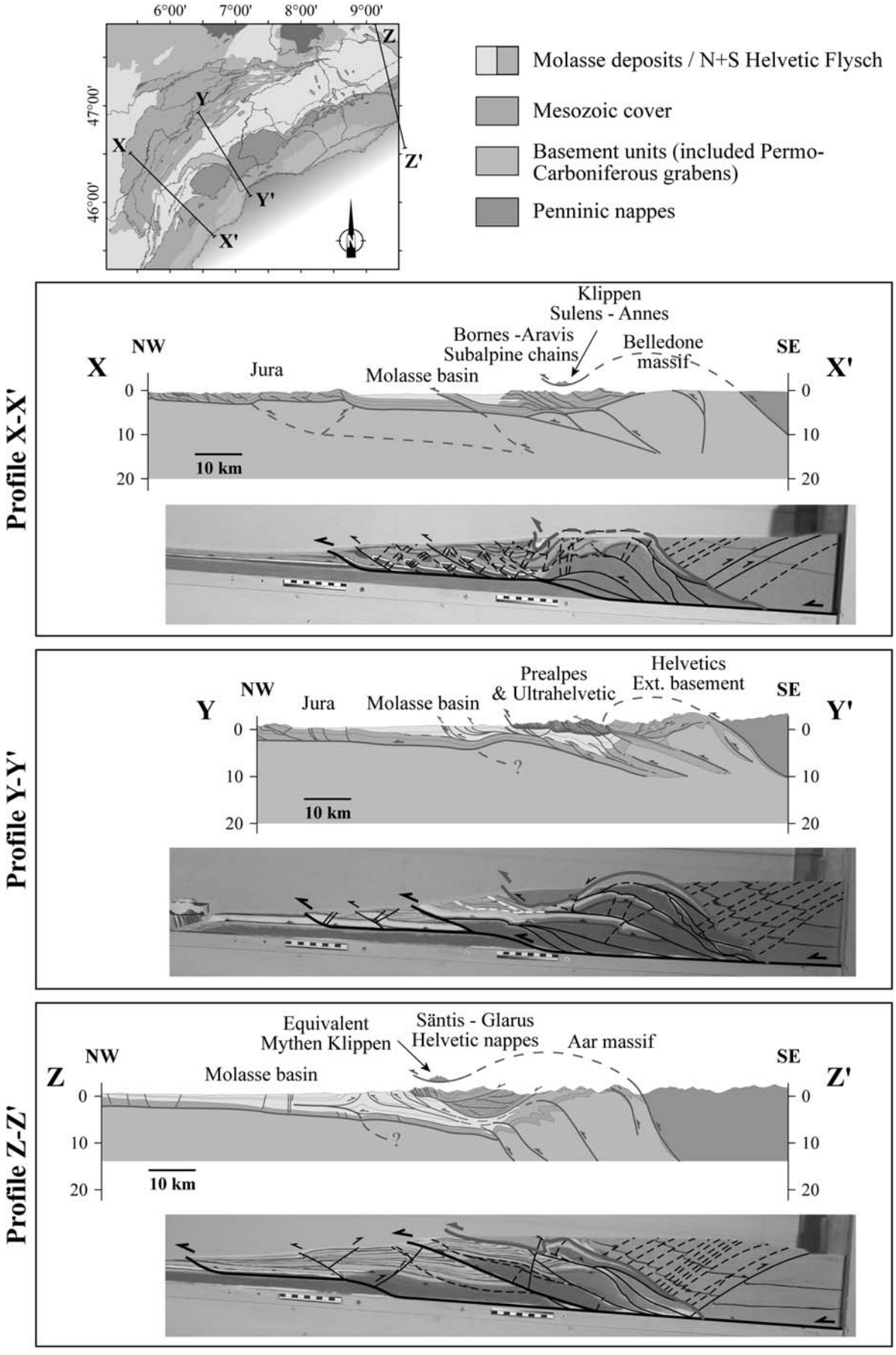

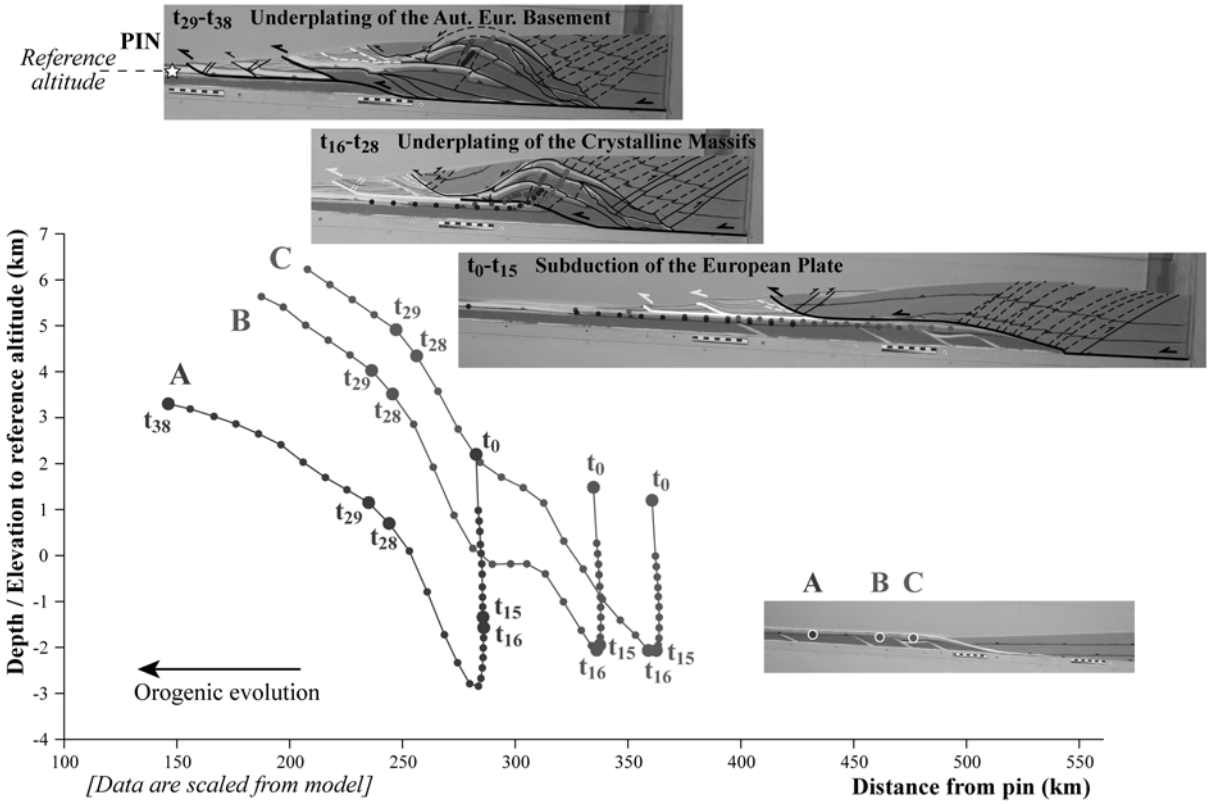

FIG. 11. – Trajectories (measured relative to a fixed reference) of three points located in the converging plate, during experiment 46. The studied points are named in reference to the Alpine setting (picture): A = top of "Infra-Rouges" massif and B = top of "Aiguilles Rouges" massif are both situated at the top of the basement units and C = Top of "Helvetic" nappes is inside the cover. The horizontal component of the movement is measured relative to a pin located in the undeformed part of the lower-plate (white star) and the vertical component to the reference altitude of the pin at the end of the experiment (dashes). Three stages of evolution appear, each one governed by a major tectonic mechanism: subduction of the lower-plate, underplating of the basement units and underplating of the homogeneous and most external part of the basement.

FIG. 11. – *Trajectoires (mesurées par rapport à une référence fixe) de trois points situés dans la plaque convergente, durant l'expérience 46. Les points étudiés sont nommés en référence à l'exemple alpin (photographie) :* A = *top of "Infra-Rouges" Massif et* B = *top of "Aiguilles Rouges" Massif sont situés au sommet des unités de socle et* C = *Top of "Helvetic" Nappes est dans la couverture. La composante horizontale du mouvement est mesurée par rapport à un point situé dans la partie non déformée de la plaque inférieure (étoile blanche) et la composante verticale par rapport à l'altitude de référence du point à la fin de l'expérience (tiretés). Trois stades d'évolution apparaissent, chacun gouverné par un mécanisme tectonique majeur : subduction de la plaque inférieure, sous-placage des unités de socle et sous-placage de la partie homogène la plus externe du socle.*

showing the exhumation paths present yet more irregularities, especially to the end, due to the variable erosion of the lid topographic surface. Another very interesting result is the timing of the events linked to the underplating. Based on the depth/elevation of the points relative to the reference altitude, the subduction phase ends at t_{15} and underplating initiates at t_{16}, by an immediate uplift of the red (B) and green (C) points. But the graph presenting the exhumation paths shows that the sedimentary thickness is still at a maximum from t_{16} to t_{18} and decreases only after this time. This discrepancy illustrates the fact that underplating and subsequent basement uplift induce a large but slightly delayed increase of the erosion rate on the lid. Changes in the slope of the "exhumation" curves (fig. 12) reflect changes in rates. Similar changes in rates of exhumation are also observed on data sets of cooling ages from the different tectonic units in the Alps [Hunziker *et al.*, 1989; Hunziker *et al.*, 1997; Kühni and Pfiffner, 2001]. Other results on uplift in the external domains of the Alps suggest rather steady exhumation [Burkhard and Goy-Eggenberger, 2001; Fuegenschuh and Schmid, 2003; Herwegh and Pfiffner, 2005]. The relative complexity of the exhumation curves from our models and the non-steadiness of the rates certainly suggest that the exhumation history may be more differentiated.

FIG. 10. – Comparison of geometrical structures between three simplified cross-sections of the central-western Alps and three analogue experiments performed with variable rates of erosion and sedimentation. Location of sections on a structural map of the western Alpine foreland: section from the Jura to the Belledonne massif (modified from Jouanne *et al.* [1995] and Lacombe and Mouthereau [2002]; Profile XX' compared with experiment 43), section from central Jura to Mont-Blanc massif (modified from Burkhard and Sommaruga [1998] and Mosar *et al.* [1996]; Profile YY' compared with experiment 46) and section from Molasse basin to Aar massif (modified from Spicher [2005]; Profile ZZ' compared with experiment 47).

FIG. 10. – *Comparaison des structures géométriques entre trois coupes simplifiées des Alpes centrales et occidentales et trois expériences analogiques réalisées avec des taux variables d'érosion et de sédimentation. Localisation des coupes: coupe du Jura au massif de Belledonne (modifié d'après Jouanne* et al. *[1995] et Lacombe et Mouthereau [2002]; profil XX' comparé avec l'expérience 43), coupe du Jura central au massif du Mont-Blanc (modifié d'après Burkhard et Sommaruga [1998] et Mosar* et al. *[1996]; profil YY' comparé avec l'expérience 46) et coupe du bassin molassique au massif de l'Aar (modifié d'après Spicher [2005]; profile ZZ' comparé avec l'expérience 47).*

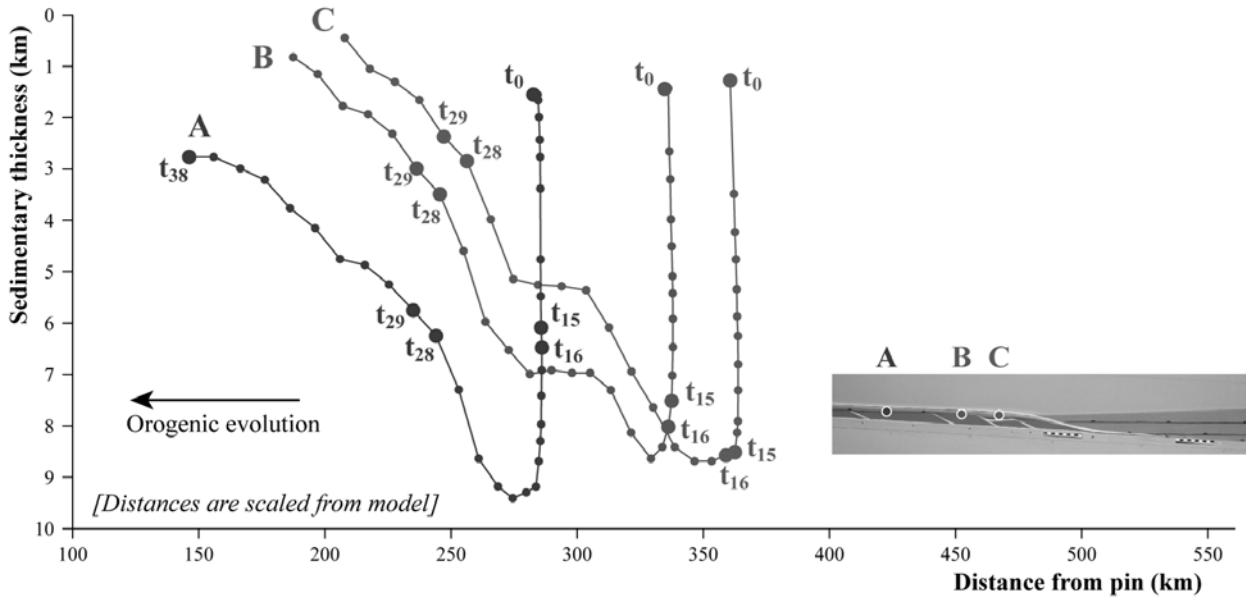

FIG. 12. – Trajectories (measured with respect to the surface) of three points located in the converging plate during experiment 46. In contrast to figure 11, the vertical component of the movement represents the distance between the study point and the surface, in terms of thickness of sediments on the analysed material. The three stages of evolution are reproduced from figure 11 (t_0 to t_{15} = subduction of the lower-plate, t_{16} to t_{28} = underplating of the basement units, t_{29} to t_{38} = underplating of the homogeneous and most external part of the basement). The uplift of basement units due to their underplating (from t_{16}) causes an increase of erosion on the lid. As the sedimentary thickness on the studied points is still maximal during some increments of displacement, it appears that the erosive response is slightly delayed.

FIG. 12. – *Trajectoires (mesurées par rapport à la surface) de trois points situés dans la plaque convergente, au cours de l'expérience 46. Contrairement à la figure 11, la composante verticale du mouvement représente la distance entre les points étudiés et la surface, en termes d'épaisseur de sédiments au-dessus du matériel analysé. Les trois stades d'évolution sont reproduits de la figure 11 (t_0 à t_{15} = subduction de la plaque inférieure, t_{16} à t_{28} = sous-placage des unités de socle, t_{29} à t_{38} = sous-placage de la partie homogène la plus externe du socle). Le soulèvement des unités de socle du fait de leur sous-placage (à partir de t_{16}) favorise une augmentation de l'érosion sur la plaque supérieure. Comme l'épaisseur sédimentaire sur les points étudiés reste maximale pendant quelques incréments de déplacement, il apparaît que la réponse érosive est légèrement décalée.*

To investigate the role of surface processes on the uplift of basement units, we studied the trajectory of a point during the experiment performed without erosion and sedimentation (experiment 42). This point is located exactly at the same position as the red one (B fig. 11) analysed in the experiment 46 (top of the second most internal basement unit) and is thus represented with the same colour (A on the scheme fig. 13). The paths of the yellow (C) and the pink (B) points located in the lid will be described in the following chapter. The trajectory of the red point (A) is simple and can be divided into two phases: from t_0 to t_{13}, the point is driven to depth quickly due to the subduction of the lower-plate and from t_{14} to t_{34}, it slightly and regularly goes up as a result of little underthrusting of the basement units.

With and without surface processes, the points located at the top of basement units in the lower-plate are first pulled to depth before going up to the surface. The initial phase is governed by the process of subduction and the second one by the underthrusting of basement units (experiment 42, fig. 13), changing to underplating (experiment 46, fig. 11) under the action of erosion. The comparison of these two experiments shows that the erosion of the lid initiates the uplift of basement units. Associated with sediment deposit in the foreland, erosion localizes and controls their exhumation with respect to the surface.

Complex uplift paths of points located in the lid

During the experiments, the converging lower-plate is underthrust below the lid upper-plate which is progressively slightly deformed by backthrusting, as its surface is gradually eroded. To better describe the evolution of the lid and estimate its internal rate of deformation, we studied the uplift paths of two inner points spatially remote (fig. 14). The most internal point (yellow point, B on scheme) is located in the core of the lid and is named "deformed Penninic landmark" in reference to the Alps and because it is largely affected by backthrusting. The second one (pink point, A) is situated close over the basal thrust of the lid, half way up the basement ramp and is named "Penninic landmark". The graph of their trajectories presents the same axis and scales as the graph showing the material paths in the lower-plate (fig. 11). While they are continuously uplifted, their paths appear to be quite different, notably during the first half of model evolution (fig. 14). Indeed, from the beginning, the external pink point (A) climbs up onto the top of the basement ramp yielding the "bump" shape of the curve, whereas the internal yellow point (B) is passively transported (t_{10}). From the stage t_{12}, the situation inverts: the internal yellow point (B) climbs up onto the top of the basement ramp and the pink one (A), having passed the ramp, is passively transported on the succession of basement units (t_{16}). In addition, the uplift of the yellow point (B) increases due to internal backthrusting deformation of the lid. The final phase is common for both points: they are passively uplifted due to basement underplating (t_{38}). However the proximity of the deformation front favours a higher uplift of the pink point (A).

In the experiment without surface processes (experiment 42), the trajectories of two points of the lid located approximately at similar places than in experiment 46

(scheme fig. 15) are comparable (fig. 15). The external point (pink, A) first climbs up the basement ramp, while the internal one (yellow, B) is passively transported (t_8). Then, the latter is also uplifted due to the combined effect of climbing up the ramp and backthrusting and the pink point (A) is passively transported on the top of basement units (t_{14}). Finally, the two points are slightly uplifted due to basement underthrusting (t_{34}). The major difference between experiments 42 and 46 is the amplitude of uplift. Without erosion (experiment 42, fig. 15), the maximal vertical displacement of the points is 6 km scaled to nature, while the value reaches 8 km when erosion is performed (experiment 46, fig. 14). The underplating of basement units, initiated by erosion, increases noticeably the uplift of the thrusting lid.

CONCLUSIONS

The series of analogue modelling experiments shows that the two main mechanisms controlling orogenic growth are cyclic frontal accretion and underplating. In the external parts of the model, frontal thrust slices are successively activated in the recently deposited foreland sediments. This frontal accretion leads to major removal of foreland basin sediments and to a consequent erosion of the inner structures accommodating displacement. This phenomenon may lead to serious underestimation of total shortening in actual mountain chains. Simultaneously in the internal zones, basement units are underthrust along weak levels simulating inherited structural control. Enhanced by erosion, this mechanism produces underplating that leads to the development of an antiformal nappe stack. This geometrical feature accommodates large displacement along very active thrust ramps.

Surface processes play a major role in the development of a mountain belt. They interact with tectonic processes to maintain the mechanical equilibrium of the wedge. The variations in rates of erosion and sedimentation strongly modify the extent, the morphology, the structures, the timing of development and the material transfer paths. For instance, erosion of the lid increases the underplating of basement units and localizes the exhumation, resulting in an antiformal nappe stack. In response, the uplift of material due to the underplating of basement units at depth leads to an increase of localized erosion. It also appears that the higher the erosion rate the steeper are the basement imbricates in the antiformal stack. However, a very high sedimentation rate in the foreland basin strongly inhibits development of an antiformal stack. In contrast, very low sedimentation rates favour the creation of a number of small thrust slices briefly active. Intermediate conditions of erosion and sedimentation lead in the foreland to the development of a sedimentary basin and a fold-and-thrust belt.

The influence of surface processes on material paths has been studied using the trajectories of three particles located in the converging lower-plate and two in the upper-plate. In the lower-plate, the complex uplift paths are

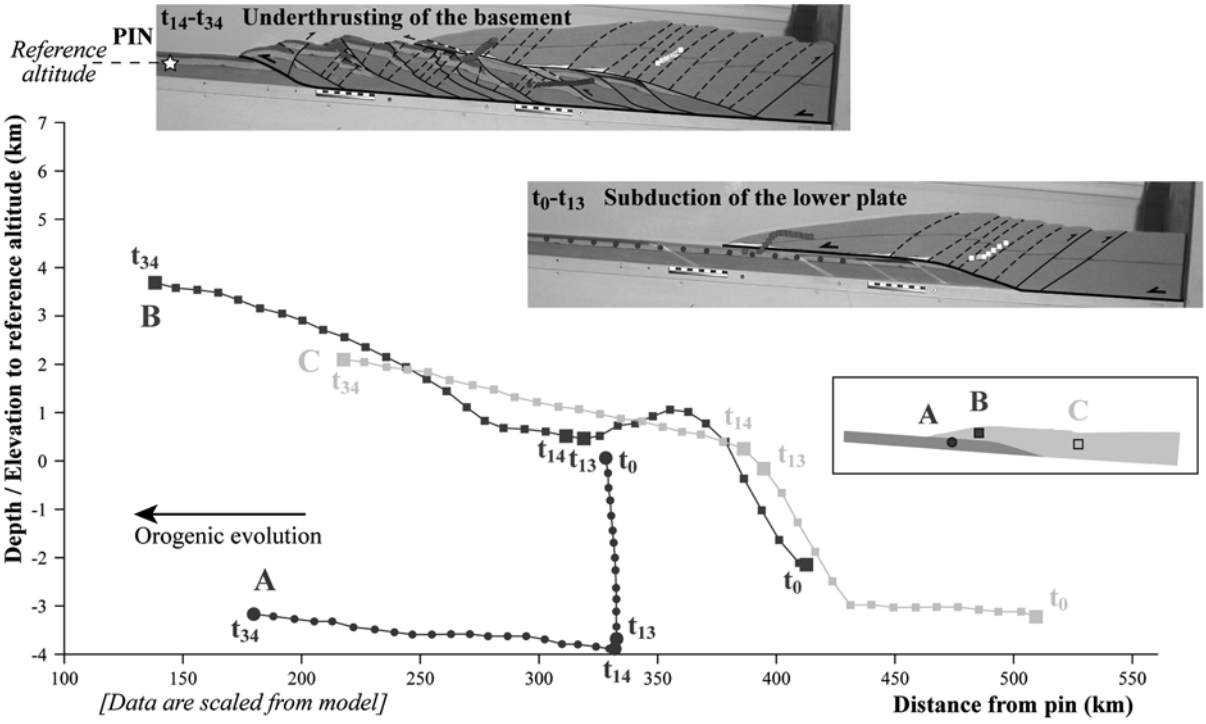

FIG. 13. – Trajectories (measured relative to a fixed reference) of one point located in the converging plate (A = top of "Aiguilles Rouges" massif) and two in the upper-plate (B = Penninic landmark and C = deformed Penninic landmark), during experiment 42 (no erosion). Trajectories are measured similarly to figure 11. The trajectory of the point in the converging plate (A) may be divided into two phases: first it goes down quickly due to the subduction of the lower-plate and then, it is slightly and regularly uplifted as a result of minor underthrusting of the basement units.

FIG. 13. – *Trajectoires (mesurées par rapport à une référence fixe) d'un point situé dans la plaque convergente (*A = *top of "Aiguilles Rouges" massif) et de deux dans la plaque supérieure (*B = *Penninic landmark and* C = *deformed Penninic landmark), pendant l'expérience 42 (sans érosion). Les trajectoires sont mesurées de la même façon que dans la figure 11. La trajectoire du point situé dans la plaque convergente (A) peut être décrite en deux étapes: le point s'enfonce rapidement en profondeur du fait de la subduction de la plaque inférieure puis il remonte lentement mais régulièrement du fait du léger chevauchement des unités de socle.*

related to the tectonic stages (subduction and underplating). In the lid, the trajectories are linked to thrusting movement of the upper-plate, before being affected by underplating of the lower-plate basement units. Two experiments performed with and without surface processes show quite similar trajectories for particles in the upper– and lower-plates. The main difference is that erosion increases the amplitude of underplating and consequently the amplitude of particle uplift. In addition, two neighbouring points may follow very dissimilar trajectories. Local differences in structures and/or lithologies may lead to major variations in the tectonic development. Studies of exhumation paths in mountain belts often show trajectories of rocks constrained by few data points only. They are probably "smoothed" model trajectories of particles likely more complex in reality, as suggested by our model results.

The role of erosion and sedimentation on the dynamics and development of the Alpine orogen and adjacent Molasse basin has been emphasised by a comparison between tectonic cross-sections and models performed with variable rates of surface processes. For instance, with low sedimentation, as in the western Alps, the foreland basin is shallow and subdivided by thrust-related anticlines into smaller sub-basins. In contrast, in the central Alps, a broader and thicker foreland basin develops because of high sedimentation and the successive layers of foreland sediment deposits are little deformed. In the experiments, new basement imbricates develop in the frontal part of the wedge that may correspond to a forward evolutionary stage of the presumed current Alpine underplating indicated by present seismic activity and measured convergence [Mosar, 1999; Calais *et al.*, 2002]. Both, in the models and along the three Alpine cross-sections, remnants of the cover lid are represented by allochthonous klippen, of various sizes depending on the erosion rate. Along strike, the Alpine basement massifs are imbricated with styles varying from simple underthrusting to underplating and with the development of an antiformal nappe stack.

Another result of models has significant implications for geologists who study active mountain belts using kinematics of active faults to obtain estimates of middle term shortening rates. During active shortening of the model wedges, most of the horizontal displacement on faults is accounted for by few very active thrusts located at the frontal part, whereas, inside the body of the wedge, faults that reach the surface are not very active and the major part of deformation is essentially accounted for by vertical movements. Such rather unexpected deformation partitioning between horizontal displacements in the external domains

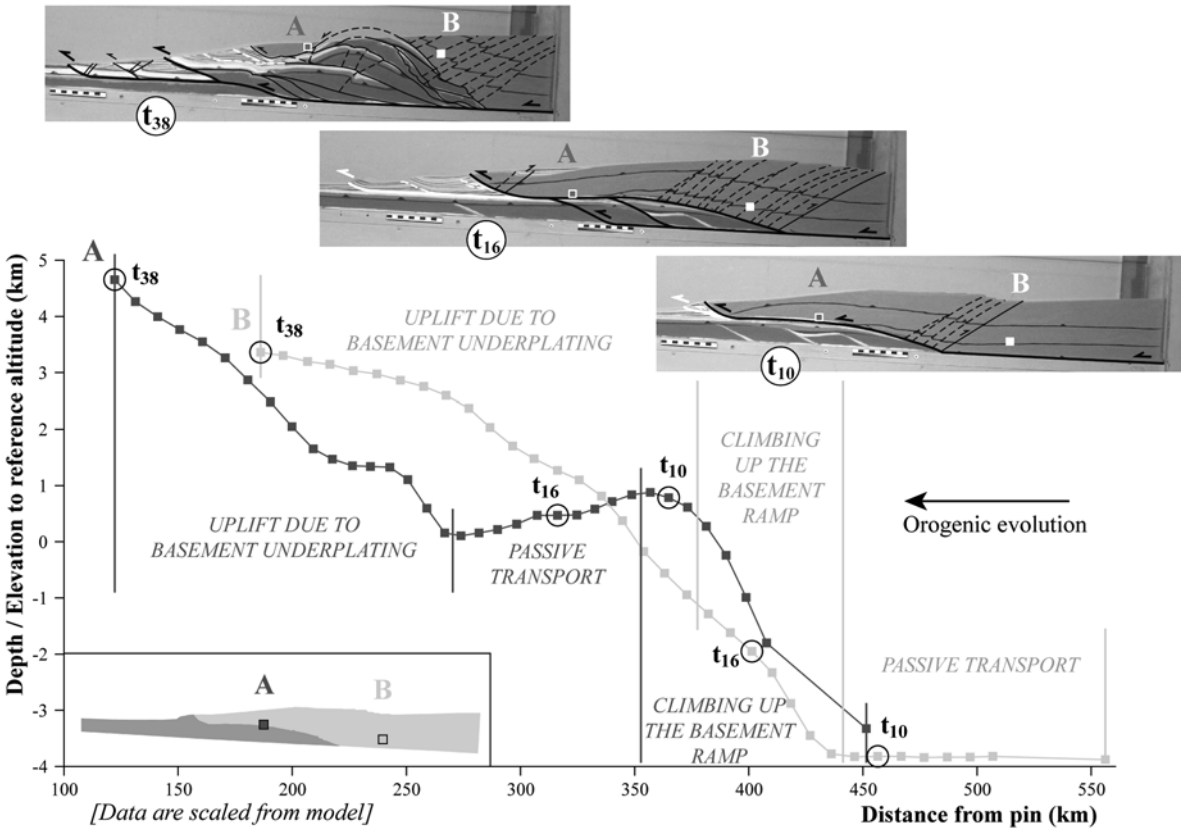

FIG. 14. – Trajectories (measured relative to a fixed reference) of two points located in the lid (A = Penninic landmark and B = deformed Penninic landmark), during experiment 46. Trajectories are measured similarly to figure 11. Point A located in the front of the lid climbs up onto the top of the basement ramp, is then passively transported on the succession of basement units and finally is uplifted due to basement underplating. Point B more internally located in the lid is passively transported, then it climbs up onto the top of the basement ramp before being passively uplifted due to basement underplating.
FIG. 14. – *Trajectoires (mesurées par rapport à une référence fixe) de deux points situés dans la plaque supérieure (*A = *Penninic landmark et* B = *deformed Penninic landmark), durant l'expérience 46. Les trajectoires sont mesurées de la même façon que dans la figure 11. Le point A situé au front de la plaque supérieure monte sur le sommet de la rampe de socle, est ensuite transporté passivement sur la succession d'unités de socle et finalement est soulevé du fait du sous-placage du socle. Le point B situé plus internement dans la plaque supérieure est passivement transporté, puis il monte sur le sommet de la rampe de socle avant d'être ensuite passivement soulevé du fait du sous-placage du socle.*

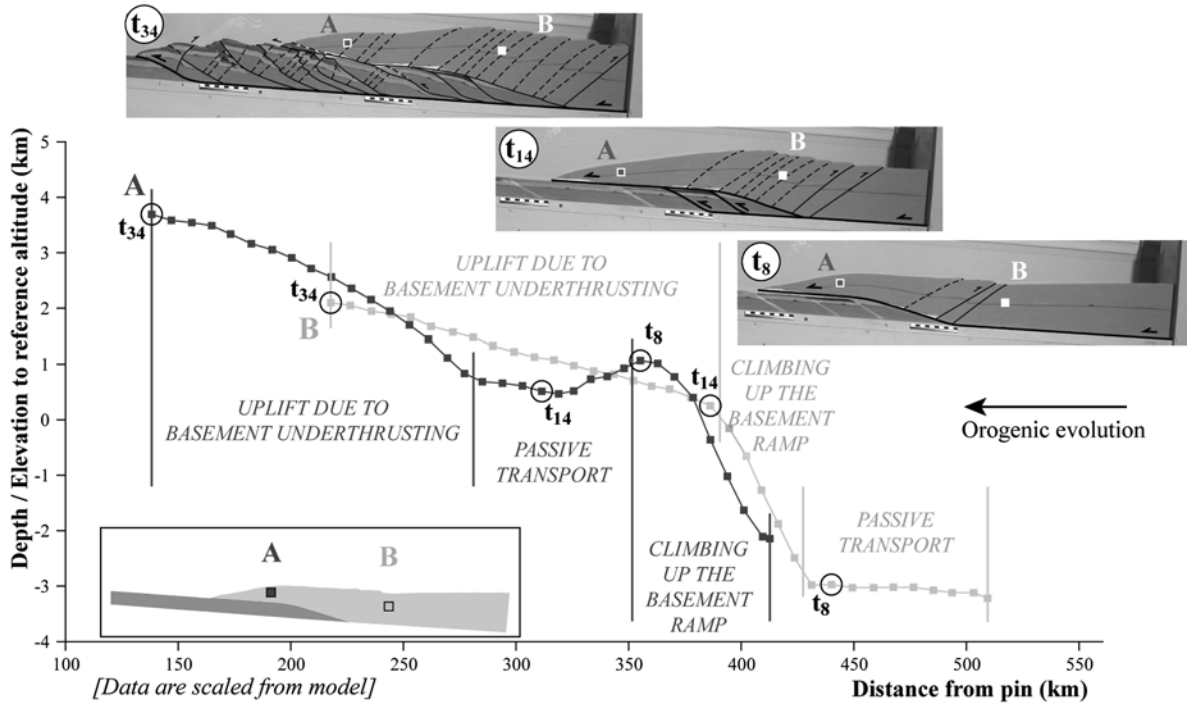

FIG. 15. – Trajectories (measured relative to a fixed reference) of two points located in the lid, experiment 42 (no erosion). Trajectories are measured similarly to figure 11. The two-dimensional trajectories of both points are similar to the trajectories described in the experiment performed with surface processes (see fig. 14). The only difference is the amplitude of uplift, increased by the underplating of basement units and therefore by erosion.
FIG. 15. – *Trajectoires (mesurées par rapport à une référence fixe) de deux points situés dans la plaque supérieure, durant l'expérience 42 (sans érosion). Les trajectoires sont mesurées de la même façon que dans la figure 11. Les trajectoires en deux dimensions des deux points sont similaires à celles décrites dans le cadre de l'expérience réalisée en simulant les processus de surface (voir fig. 14). La seule différence est l'amplitude du soulèvement, accrû par le sous-placage des unités de socle et par conséquent par l'érosion.*

and vertical movements in the inner parts of the wedge is a direct consequence of simultaneous frontal accretion and underplating at depth. These mechanisms seem to have occurred both in fossil orogens (for example the Alps, this study) and in active mountain belts, such as Taiwan [e.g., Simoes *et al.*, 2006] and the Himalaya [e.g., Avouac, 2003].

Acknowledgements. – This paper is the result of PhD research performed jointly at the Universities of Montpellier, France and Fribourg, Switzerland and supported by the University of Fribourg and by a grant of "cotutelle de thèse" (dual PhD) from the Ministère délégué à l'Enseignement supérieur et à la Recherche (France). Insightful and constructive reviews by Marc-André Gutscher and Michel Faure significantly improved the manuscript. We dedicate this paper to the memory of Martin Burkhard.

References

AVOUAC J.-P. (2003). – Mountain building, erosion, and the seismic cycle in the Nepal Himalaya. – *Advances in Geophysics*, **46**, 1-80.

BEAUMONT C., FULLSACK P. & HAMILTON J. (1992). – Erosional control of active compressional orogens. *In*: K. R. MCCLAY, Ed., Thrust tectonics. – Chapman & Hall, London, 1-18.

BONNET C. (2007). – Interactions between tectonics and surface processes in the Alpine foreland: Insights from analogue model and analysis of recent faulting. – PhD thesis, University of Fribourg, 189 p.

BURKHARD M. & GOY-EGGENBERGER D. (2001). – Near vertical iso-illite-crystallinity surfaces cross-cut the recumbent fold structure of the Morcles nappe, Swiss Alps. – *Clay Minerals*, **36**, 159-170.

BURKHARD M. & SOMMARUGA A. (1998). – Evolution of the Swiss Molasse basin: structural relations with the Alps and the Jura belt. – *Geol. Soc. London Sp. Publ.*, **134**, 279-298.

CALAIS E., NOCQUET J.-M., JOUANNE F. & TARDY M. (2002). – Current strain regime in the western Alps from continuous GPS measurements, 1996-2001. – *Geology*, **30**, 7, 651-654.

DAHLEN F.A. (1984). – Noncohesive critical Coulomb wedges: an exact solution. – *J. Geophys. Res.*, **89**, 10125-10133.

DAHLEN F.A., SUPPE J. & DAVIS D.M. (1984). – Mechanics of fold and thrust belts and accretionary wedges: cohesive Coulomb theory. – *J. Geophys. Res.*, **89**, 10087-10101.

DAVIS D.M., SUPPE J. & DAHLEN F.A. (1983). – Mechanics of fold and thrust belts and accretionary wedges. – *J. Geophys. Res.*, **88**, 1153-1172.

ENGLAND P. & MOLNAR P. (1990). – Surface uplift, uplift of rocks, and exhumation of rocks. – *Geology*, **18**, 1173-1177.

FOSTER D.A. & JOHN B.E. (1999). – Quantifying tectonic exhumation in an extensional orogen with thermochronology: examples from the southern Basin and Range Province. – *Geol. Soc. London Sp. Publ.*, **154**, 343-364.

FUEGENSCHUH B. & SCHMID S.M. (2003). – Late stages of deformation and exhumation of an orogen constrained by fission-track data: a case study in the western Alps. – *Geol. Soc. Amer. Bull.*, **115**, 11, 1425-1440.

FUNK H. & LOUP B. (1992). – Mesozoic subsidence analysis from the Jura to the Helvetic realm. – *Eclogae Geol. Helv.*, **85**, 3, 774-775.

GUTSCHER M.-A., KUKOWSKI N., MALAVIEILLE J. & LALLEMAND S. (1996). – Cyclical behavior of thrust wedges: Insights from high basal friction sandbox experiments. – *Geology*, **24**, 2, 135-138.

GUTSCHER M.-A., KUKOWSKI N., MALAVIEILLE J. & LALLEMAND S. (1998). – Episodic imbricate thrusting and underthrusting: Analog experiments and mechanical analysis applied to the Alaskan accretionary wedge. – *J. Geophys. Res.*, **103**, B5, 10,161-10,176.

HERWEGH M. & PFIFFNER O.A. (2005). – Tectono-metamorphic evolution of a nappe stack: A case study of the Swiss Alps. – *Tectonophysics*, **404**, 1-2, 55-76.

HOMEWOOD P. (1986). – Geodynamics and paleogeography of the western Molasse basin: a review. – *Giornale di Geologia, ser. 3a*, **48**, 1, 275-284.

HOOKE R.L. (2003). – Time constant for equilibration of erosion with tectonic uplift. – *Geology*, **31**, 7, 621-624.

HORTON B.K. (1999). – Erosional control on the geometry and kinematics of thrust belt development in the central Andes. – *Tectonics*, **18**, 1292-1304.

HOTH S., ADAM J., KUKOWSKI N. & ONCKEN O. (2004). – Influence of erosion on the kinematics of bivergent orogens. Results from scaled sandbox-simulations. – *Geol. Soc. Amer. Sp. Paper*, **398**, 201-225.

HUNZIKER J.C., DESMOND J. & MARTINOTTI G. (1989). – Alpine thermal evolution in the central and western Alps. *In*: M.P. COWARD, D. DIETRICH & R.G. PARK, Eds., Alpine tectonics. – *Geol. Soc. Sp. Publ.*, **45**, 353-367.

HUNZIKER J.C., HURFORD A.J. & CALMBACH L. (1997). – Alpine cooling and uplift. *In*: O. A. PFIFFNER, P. LEHNER, P. Z. HEITZMAN, S. MUELLER & A. STECK, Eds., Deep structure of the Swiss Alps – Results from NRP 20. – Birkhäuser AG., Basel, 260-263.

JOUANNE F., MÉNARD G. & DARMENDRAIL X. (1995). – Present-day vertical displacements in the northwestern Alps and the southern Jura Mountains: Data from leveling comparisons. – *Tectonics*, **14**, 3, 606-616.

KONSTANTINOVSKAIA E. & MALAVIEILLE J. (2005). – Erosion and exhumation in accretionary orogens: Experimental and geological approaches. – *Geochem., Geophys., Geosyst.*, **6**, 2, Q02006, doi: 10.1029/2004GC000794.

KUHLEMANN J. (2000). – Post-collisional sediment budget of circum-Alpine basins (Central Europe). – *Mem. Soc. Geol. Padova*, **52**, 1-91.

KUHLEMANN J., FRISCH W., DUNKL I. & SZÉKELY B. (2001). – Quantifying tectonic versus erosive denudation by the sediment budget: the Miocene core complexes of the Alps. – *Tectonophysics*, **330**, 1-23.

KUHLEMANN J., FRISCH W., SZÉKELY B. & DUNKL I. (2002). – Post-collisional sediment budget history of the Alps: tectonic versus climatic control. – *Internat. J. Earth Sci.*, **91**, 818-837.

KÜHNI A. & PFIFFNER O.A. (2001). – Drainage patterns and tectonic forcing: a model study for the Swiss Alps. – *Basin Res.*, **13**, 169-197.

KUKOWSKI N., LALLEMAND S., MALAVIEILLE J., GUTSCHER M.-A. & RESTON T.J. (2002). – Mechanical decoupling and basal duplex formation observed in sandbox experiments with application to the Mediterranean ridge accretionary complex. – *Mar. Geol.*, **186**, 29-42.

LACOMBE O. & MOUTHEREAU F. (2002). – Basement-involved shortening and deep detachment tectonics in forelands of orogens: Insights from recent collision belts (Taiwan, western Alps, Pyrenees). – *Tectonics*, **21**, 4, 1-22.

LALLEMAND S., SCHNURLE P. & MALAVIEILLE J. (1994). – Coulomb theory applied to accretionary and non-accretionary wedges – Possible causes for tectonic erosion and/or frontal accretion. – *J. Geophys. Res.*, **99**, B6, 12033-12055.

LOHRMANN J., KUKOWSKI N., ADAM J. & ONCKEN O. (2003). – The impact of analogue material properties on the geometry, kinematics and dynamics of convergent sand wedges. – *J. Struct. Geol.*, **25**, 1691-1711.

MALAVIEILLE J. (1984). – Modélisation expérimentale des chevauchements imbriqués: application aux chaînes de montagnes. – *Bull. Soc. géol. Fr.*, 7, **XXVI**, 1, 129-138.

MOSAR J. (1999). – Present-day and future tectonic underplating in the western Swiss Alps: reconciliation of basement/wrench-faulting and décollement folding of the Jura and Molasse basin in the Alpine foreland. – *Earth Planet. Sci. Lett.*, **173**, 3, 143-145.

MOSAR J., STAMPFLI G.M. & GIROD F. (1996). – Western Préalpes médianes: timing and structure. A review. – *Eclogae Geol. Helv.*, **89**, 1, 389-425.

NAYLOR M., SINCLAIR H.D., WILLET S. & COWIE P.A. (2005). – A discrete element model for orogenesis and accretionary wedge growth. – *J. Geophys. Res.*, **110**, B12403, doi: 10.1029/2003JB002940.

PERSSON K.S. & SOKOUTIS D. (2002). – Analogue models of orogenic wedges controlled by erosion. – *Tectonophysics*, **356**, 323-336.

PFIFFNER O.A., ELLIS S. & BEAUMONT C. (2000). – Collision tectonics in the Swiss Alps: Insight from geodynamic modeling. – *Tectonics*, **19**, 6, 1065-1094.

PLATT J.P. (1986). – Dynamics of orogenic wedges and the uplift of high-pressure metamorphic rocks. – *Geol. Soc. Amer. Bull.*, **97**, 1037-1053.

SCHLUNEGGER F. & HINDERER M. (2001). – Crustal uplift in the Alps: why the drainage pattern matters. – *Terra Nova*, **13**, 425-432.

SIMOES M., AVOUAC J.-P., BEYSSAC O., GOFFÉ B., FARLEY K. & CHEN Y.-G. (2006). – Mountain-building in Taiwan: a thermo-kinematic model. – *J. Geophys. Res.* (in press).

SINCLAIR H.D. (1997). – Flysch to molasse transition in peripheral foreland basins: The role of the passive margin versus slab breakoff. – *Geology*, **25**, 12, 1123-1126.

SISSINGH W. (1997). – Tectonostratigraphy of the North Alpine foreland basin: correlation of tertiary depositional cycles and orogenic phases. – *Tectonophysics*, **282**, 223-256.

SISSINGH W. (2006a). – Kinematic sequence stratigraphy of the European Cenozoic rift system and Alpine foreland basin: correlation with Mediterranean and Atlantic plate-boundary events. – *Neth. J. Geosci.*, **85**, 2, 77-129.

SISSINGH W. (2006b). – Syn-kinematic palaeogeographic evolution of the West European platform: correlation with Alpine plate collision and foreland deformation. – *Neth. J. Geosci.*, **85**, 2, 131-180.

SPICHER A. (2005). – Carte tectonique de la Suisse à 1/500 000. Mise à jour 2005. – Wabern: Office fédéral des eaux et de la géologie.

STAMPFLI G.M. & MARTHALER M. (1990). – Divergent and convergent margins in the northwestern Alps confrontation to actualistic models. – *Geodin. Acta*, **4**, 3, 159-184.

STAMPFLI G.M., BOREL G.D., MARCHANT R. & MOSAR J. (2002). – Western Alps geological constraints on western Tethyan reconstructions. – *The Virtual Explorer – http : //virtualexplorer.com.au*, **8**, 75-104.

STAMPFLI G.M., MOSAR J., MARCHANT R., MARQUER D., BAUDIN T. & BOREL G. (1998). – Subduction and obduction processes in the Swiss Alps. – *Tectonophysics*, **296**, 159-204.

SUMMERFIELD M.A. & HULTON N.J. (1994). – Natural controls of fluvial denudation rates in major drainage basins. – *J. Geophys. Res.*, **99**, 7, 13871-13883.

TRÜMPY R. (1980). – Geology of Switzerland: a guide-book. – Wepf. and Co., Basel, 334.

WILDI W., FUNK H.P., LOUP B., AMATO E. & HUGGENBERGER P. (1989). – Mesozoic subsidence history of the European marginal shelves of Alpine Tethys (Helvetic realm, Swiss Plateau and Jura). – *Eclogae Geol. Helv.*, **82**, 3, 817-840.

WILLETT S., BEAUMONT C. & FULLSACK P. (1993). – Mechanical model for the tectonics of doubly-vergent compressional orogens. – *Geology*, **21**, 4, 371-374.

WILLETT S.D. & BRANDON M.T. (2002). – On steady states in mountain belts. – *Geology*, **2**, 175-178.